The Probabilistic Two-Phase Wake Vortex Decay and Transport Model – Recent Developments and Applications

Frank Holzäpfel

Institut für Physik der Atmosphäre
Deutsches Zentrum für Luft- und Raumfahrt
Oberpfaffenhofen

- P2P model design
- comparison with field measurement data and other models
- P3P
- applications / use in wake vortex systems

DLR Deutsches Zentrum für Luft- und Raumfahrt e.V.
in der Helmholtz-Gemeinschaft

DLR

wake-vortex real-time model – requirements

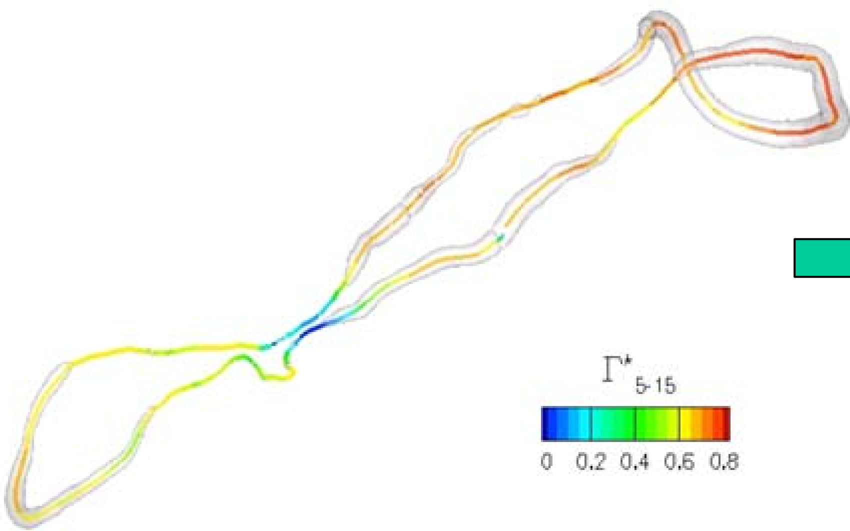

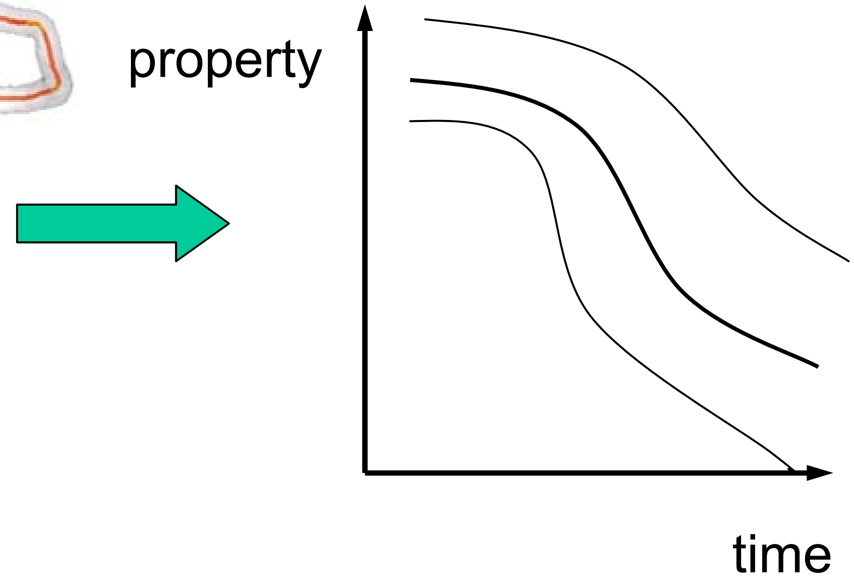

fast

robust

accurate

reliable

consider stochastic WV properties

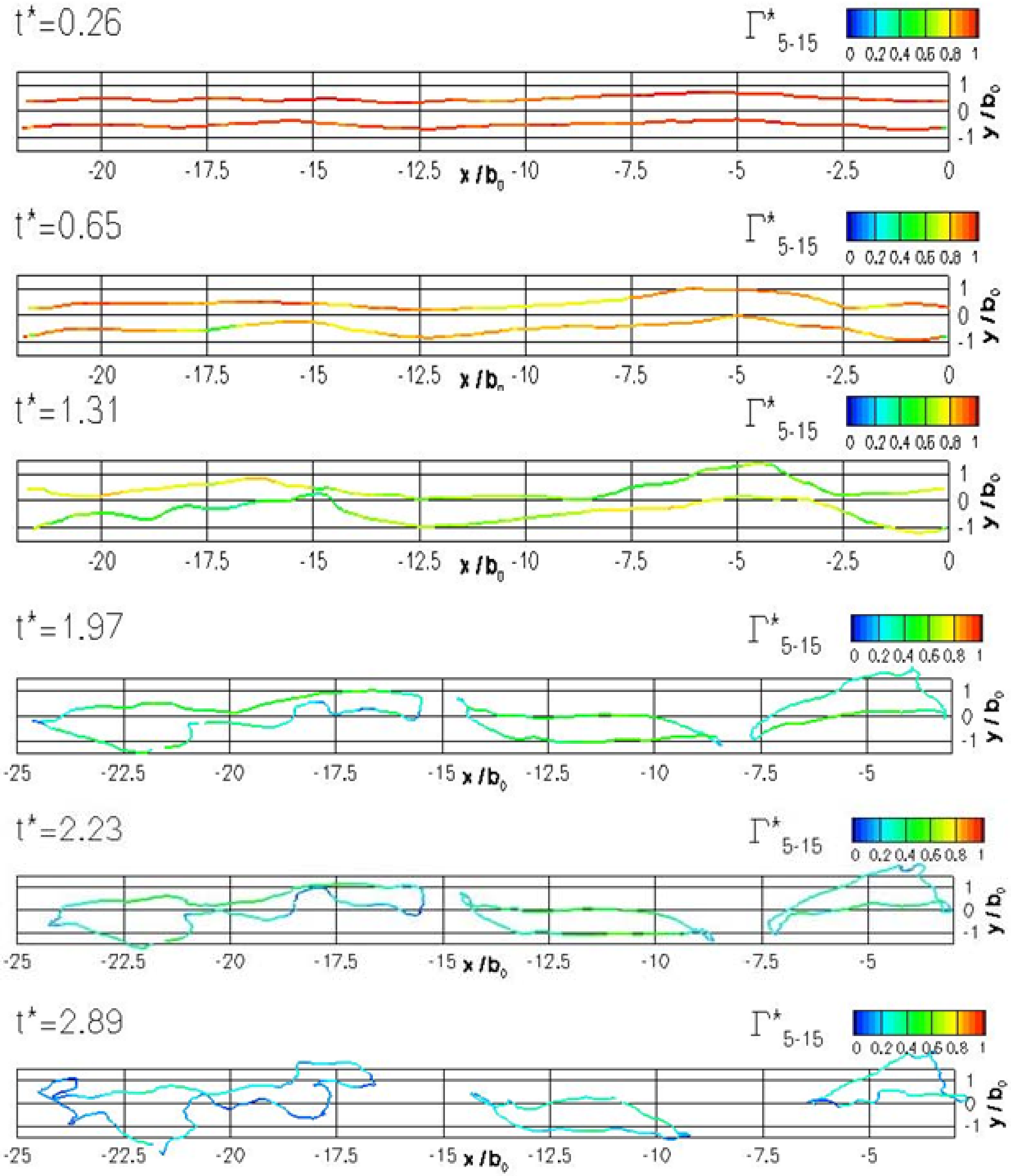

vortex topology large domain

$1024 \times 1024 \times 1024$ m³

$\varepsilon^* = 0.4$, $N^* = 0$, $L_t^* = 2.2$

Ingo Hennemann

P2P – Concept

Four pillars of P2P wake vortex model:

- dimensional analysis - characteristic scales: b_0, $t_0 = 2\pi\, b_0^2/\Gamma_0 = b_0/w_0$
- hydrodynamic basis -
  laminar decaying potential vortex
  $$\frac{\Gamma(r,t)}{\Gamma_0} = 1 - \exp\frac{-r^2}{4\upsilon t}$$
- adjustment to LES results of different groups
- calibration with field measurement data ⇒ prediction of pdfs

…

- well defined circulation: Γ_{5-15}

parameters

P2P accounts for effects of three components of wind,
axial- and crosswind shear, turbulence,
stable thermal stratification, and ground proximity

input data:
- a/c: $x_0, y_0, z_0, t_0, V, m, b, \gamma, \psi, \phi$
- meteo: $u(z), v(z), (w(z)), \rho(z_0), q(z), \varepsilon(z), \theta(z)$

output data: $\Gamma(t) \pm \Delta\Gamma(t)$, $y(t) \pm \Delta y(t)$, $z(t) \pm \Delta z(t)$, [$r_c(t)$, pdfs of $\gamma(t)$, $\psi(t)$, $\phi(t)$] at a certain flight path position (gate)

model equations — two-phase decay

$$\Gamma^*_{5-15}(t^*) = A - \underbrace{\exp\frac{-R^{*2}}{\nu_1^*(t^*-T_1^*)}}_{diffusion} - \exp\frac{-R^{*2}}{\nu_2^*(t^*-T_2^*)}$$

rapid decay

onset of rapid decay

respective decay rate

= f (ε*, N*, z*)

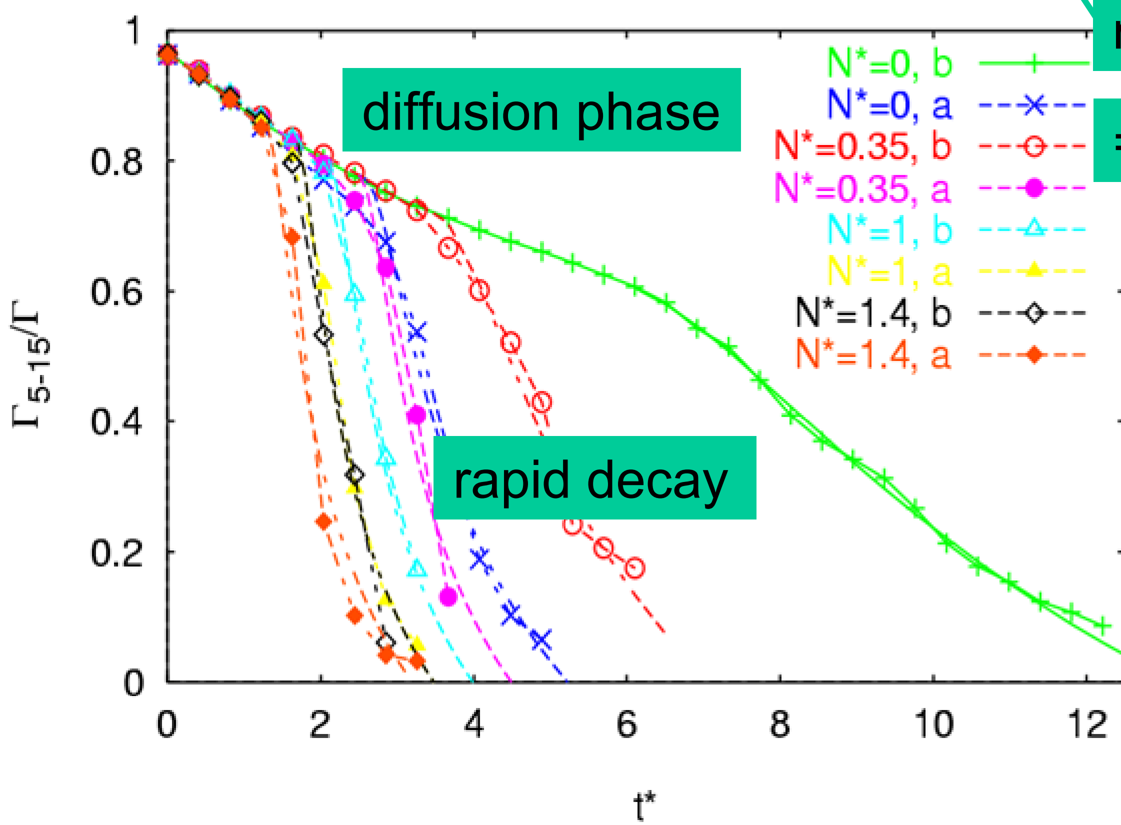

lidar — two-phase decay

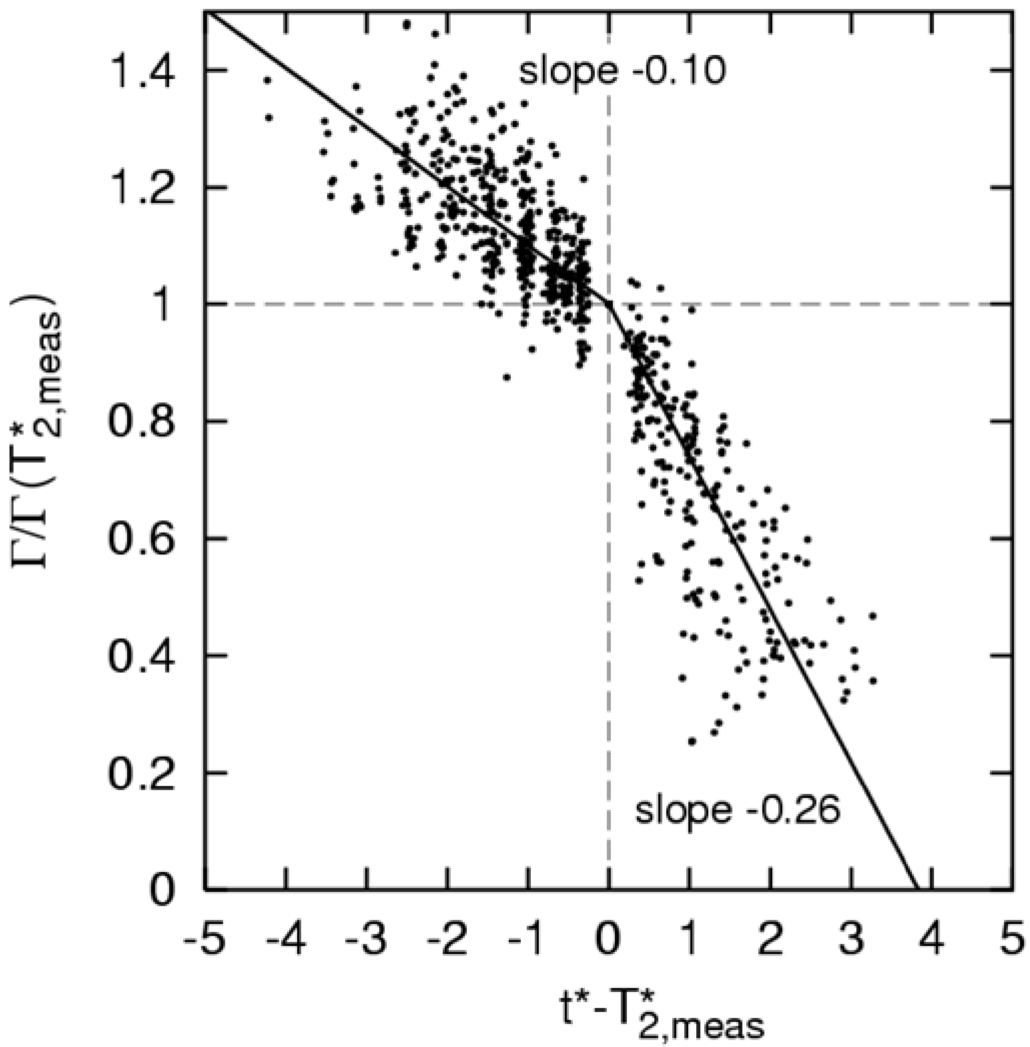

onset of rapid decay T_2^* (OGE)

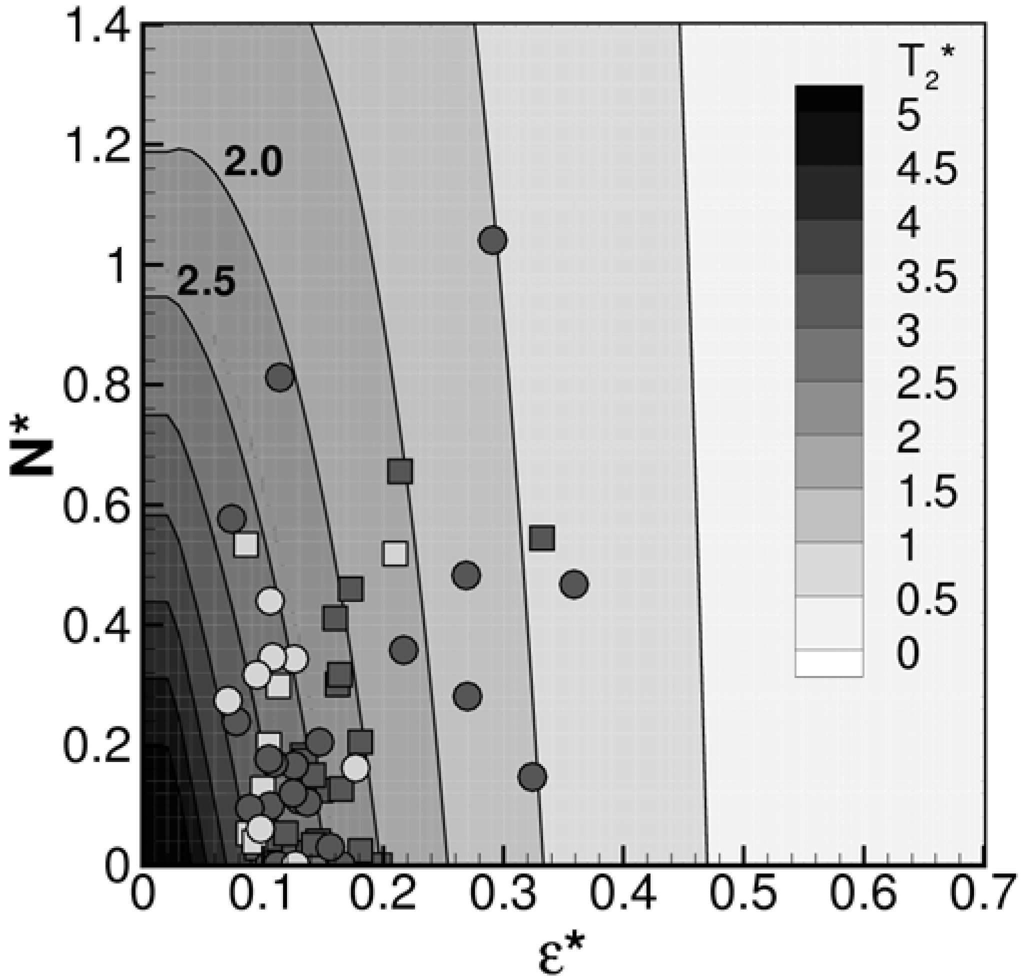

Sarpkaya, J. Aircraft **37** 2000
Holzäpfel, J. Aircraft **43** 2006

descent speed

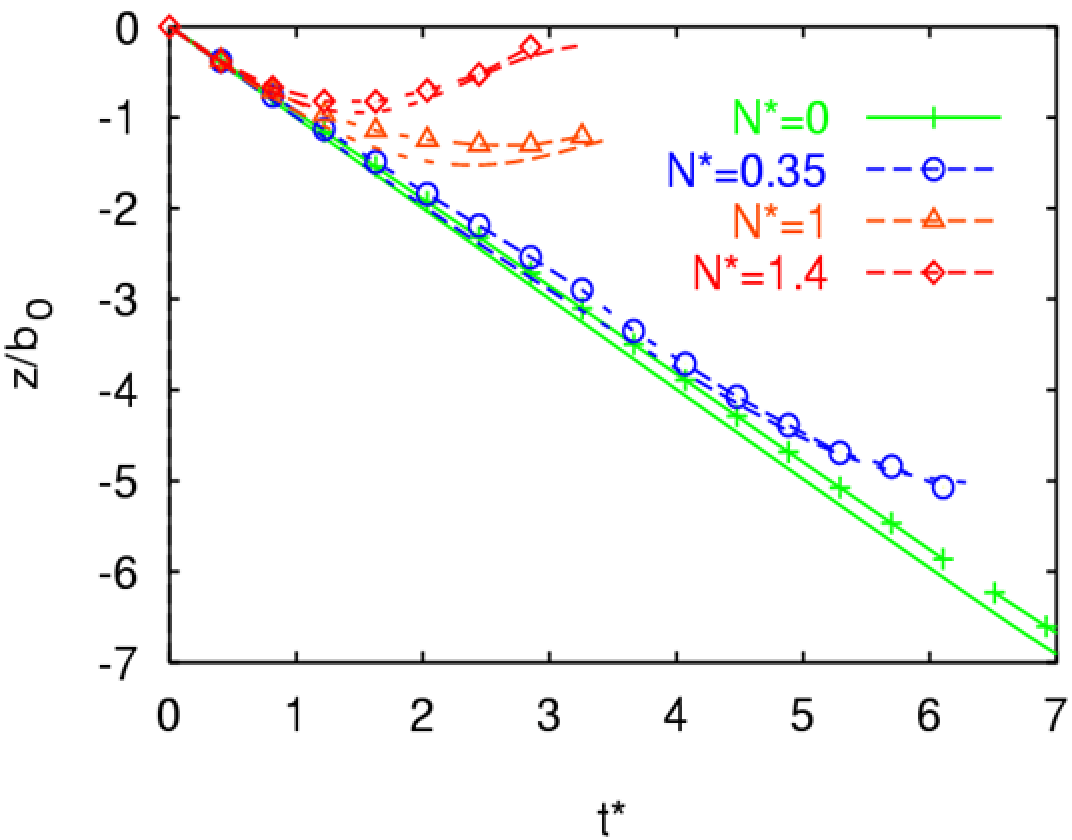

non-linear relation between circulation and descent speed

⇒ stagnating or even re-bounding vortices in strongly stably stratified environment

crosswind shear gradients

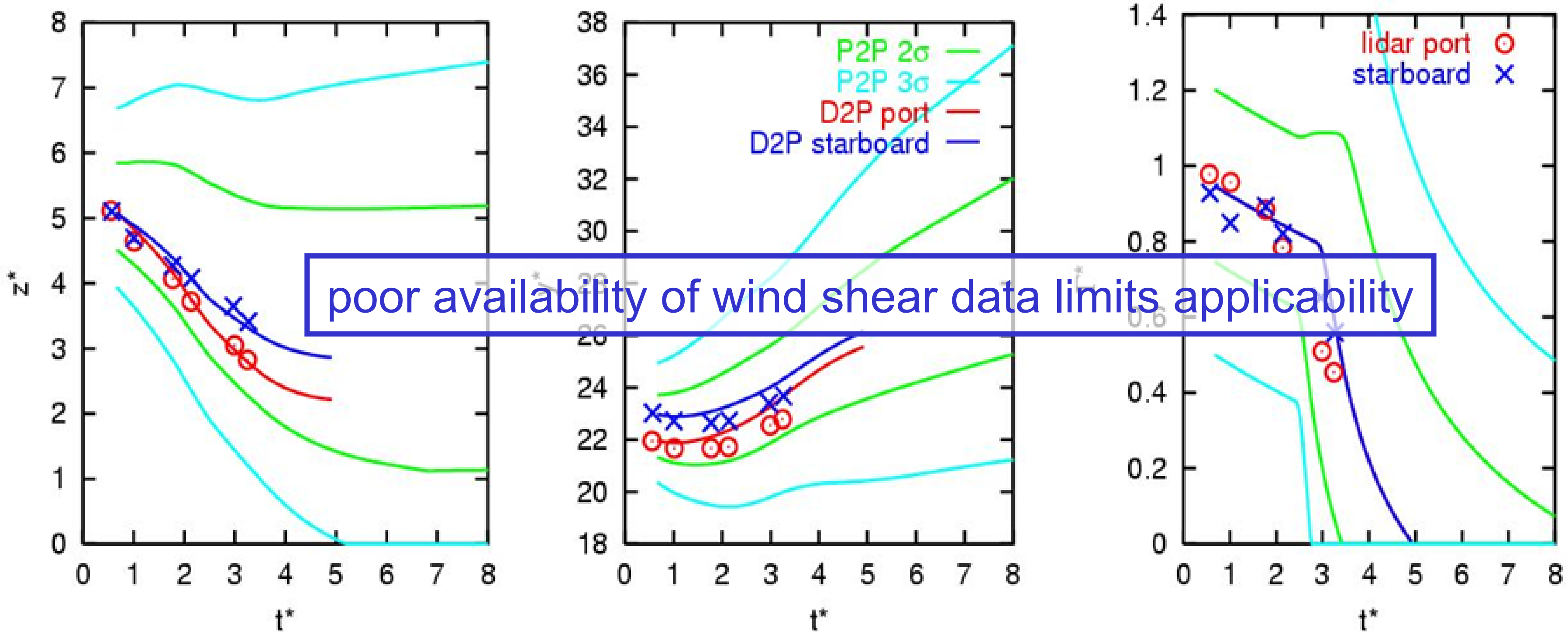

poor availability of wind shear data limits applicability

$$\frac{\partial \Gamma^*}{\partial t^*} = 1.42\ C(\Gamma^*)\, w^*\, \frac{\partial^2 v^*(z^*)}{\partial z^{*2}}$$

only for transport and only for $\frac{\partial \Gamma^*}{\partial t^*} < 0$

Delisi & Robins AIAA Papers 2006-1075/1076

ground effect with crosswind

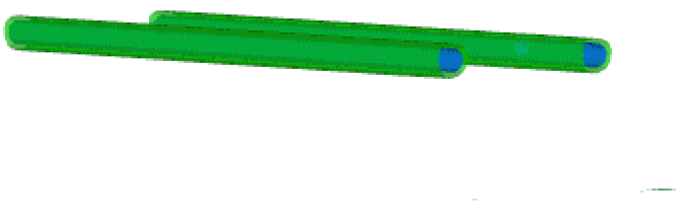

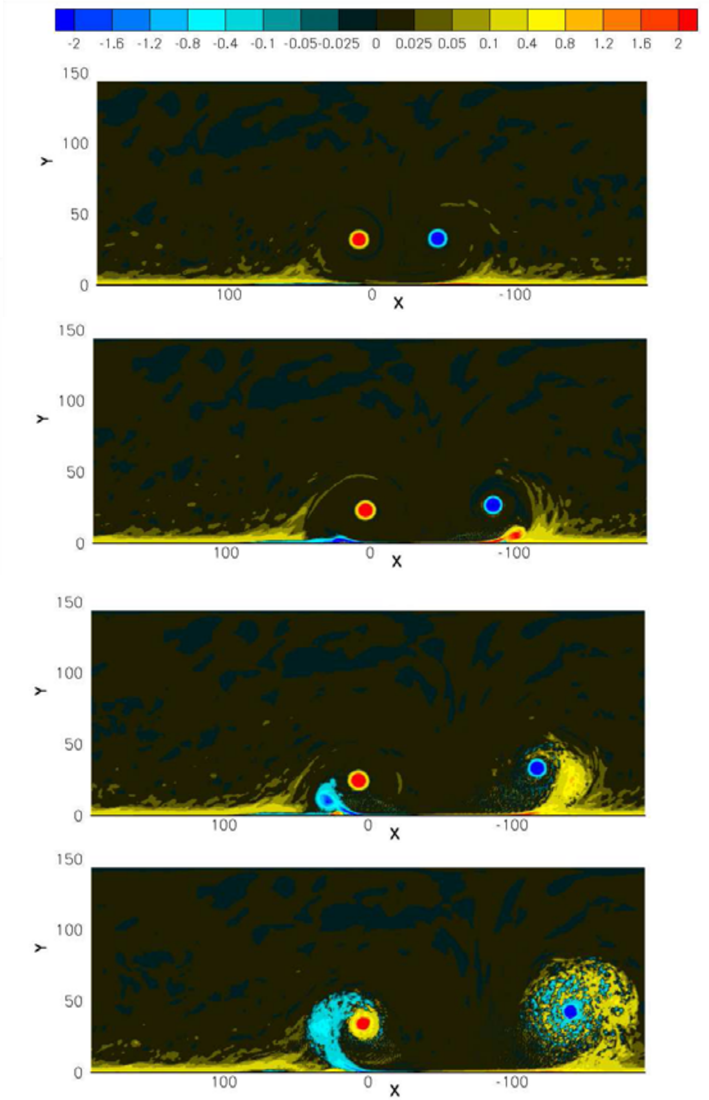

LES Anton Stephan

ground effect w/o crosswind[1]

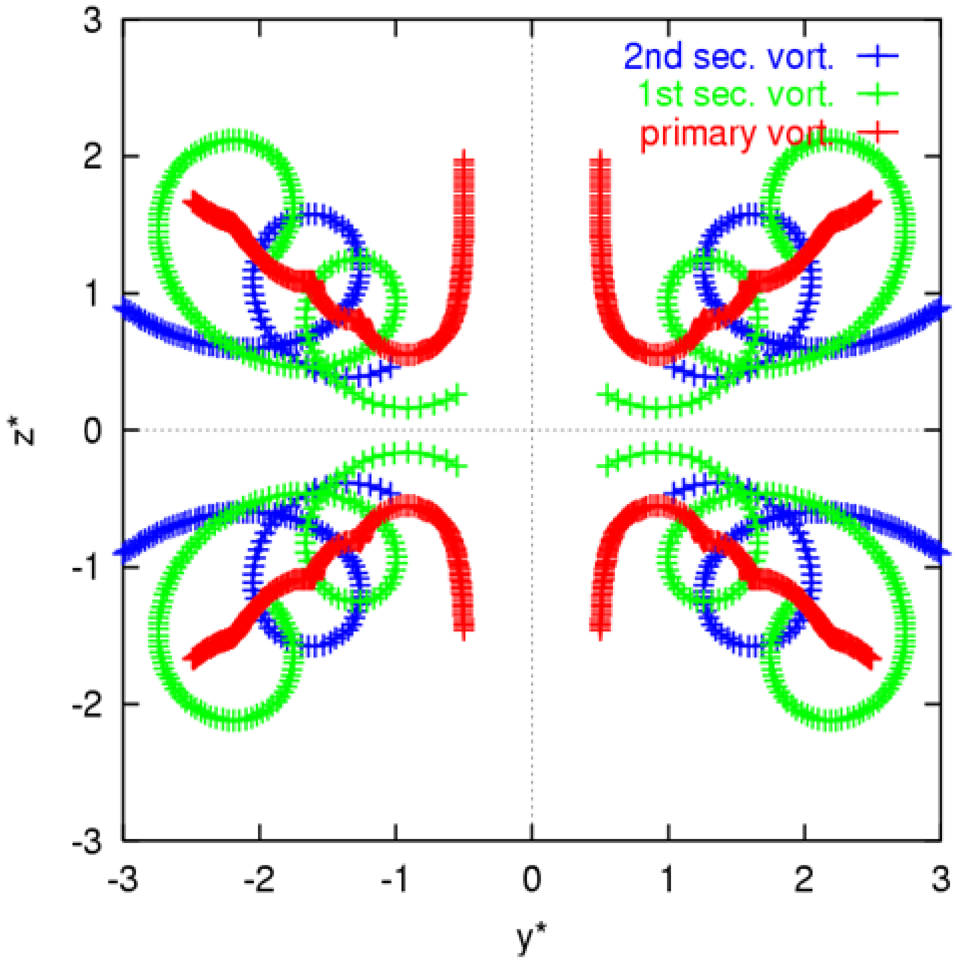

- Image vortices at z = 1.5 b_0
- GE vortices + images at z = 0.6 b_0
- after rotation of 180 deg another pair of secondary vortices + images
- $\Gamma^*_{s,max} = 0.4 w^*$

[1]Robins, Delisi, & Greene, Journal of Aircraft **38** 2001.

asymmetric rebound in crosswind conditions

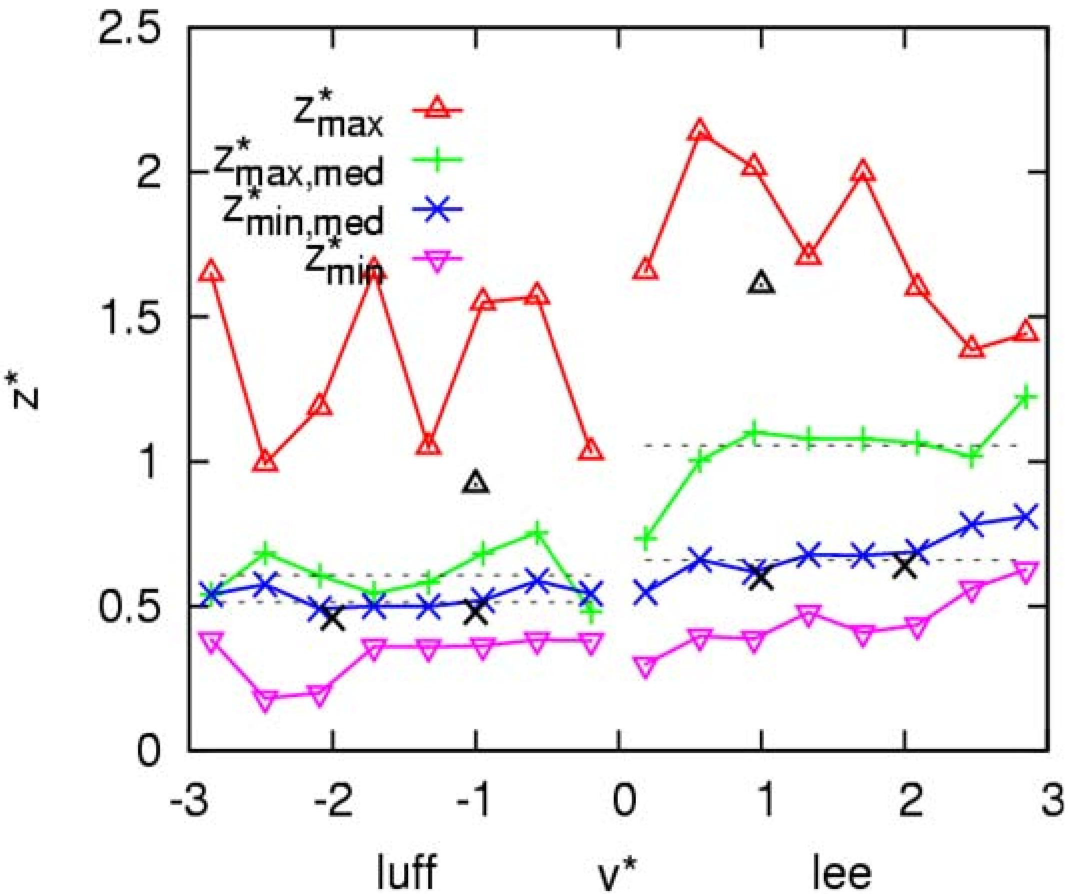

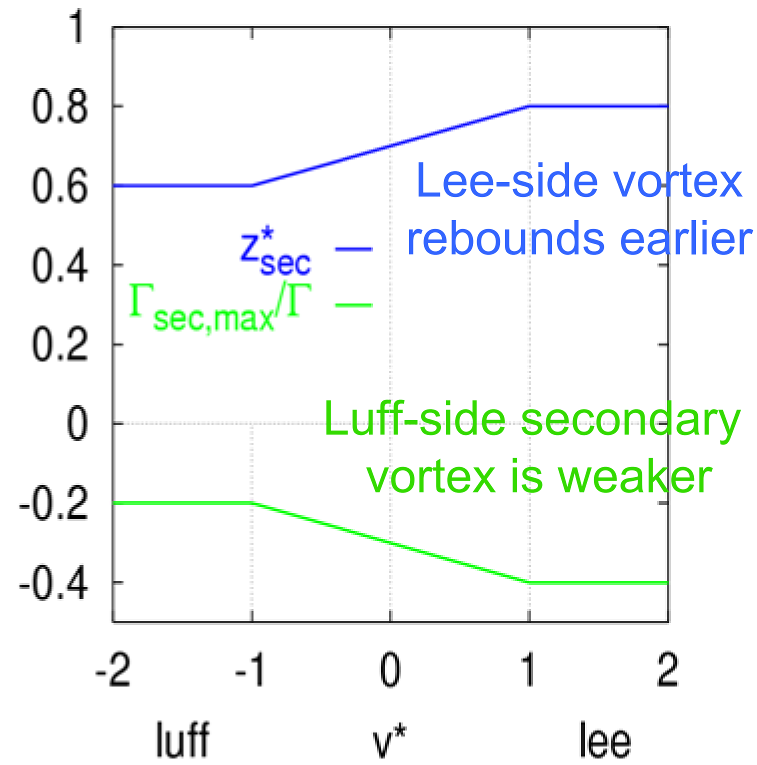

lidar 231 cases / 5210 obs.
(Holzäpfel & Steen AIAA J. 2007)
black symbols: LES of Giovannini et al.
(UPS-IMFT, CENEARO, UCL)

adapted secondary
vortex parameters

circulation decay in ground proximity

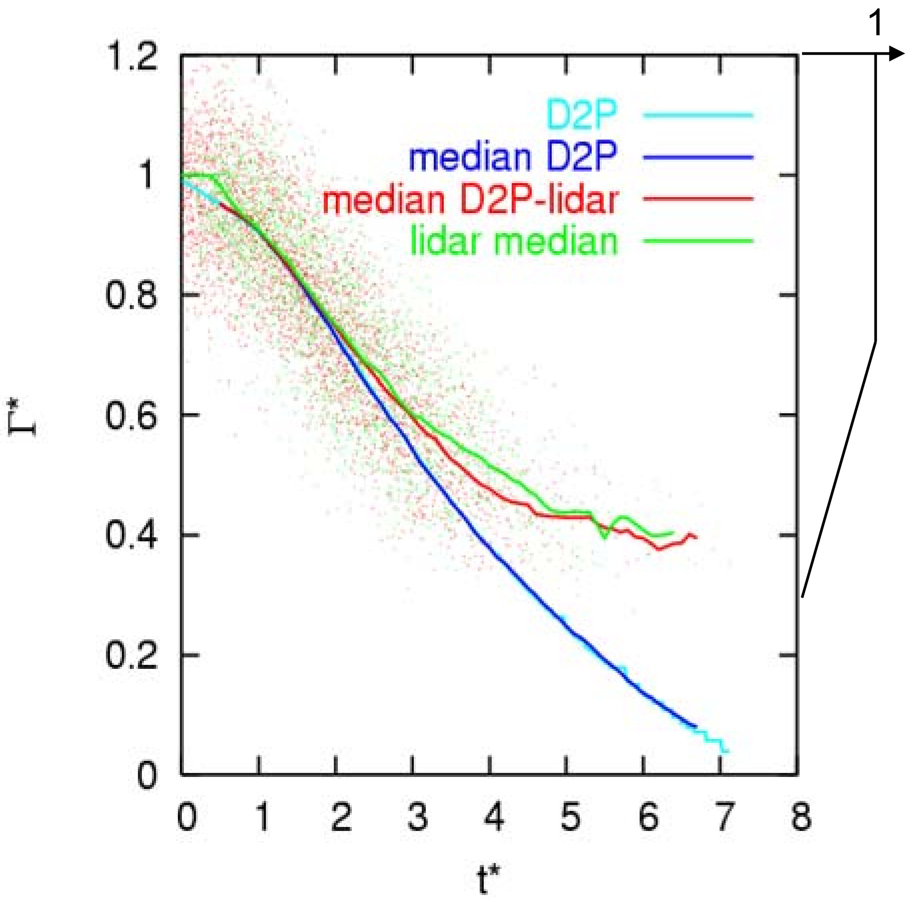

parameterization of P2P:

- onset of rapid decay 0.2 t_0 after reaching z_{min}
- decay rate adjusted to $\nu_2^* = 0.003$

Holzäpfel & Steen, AIAA J. **45** 2007

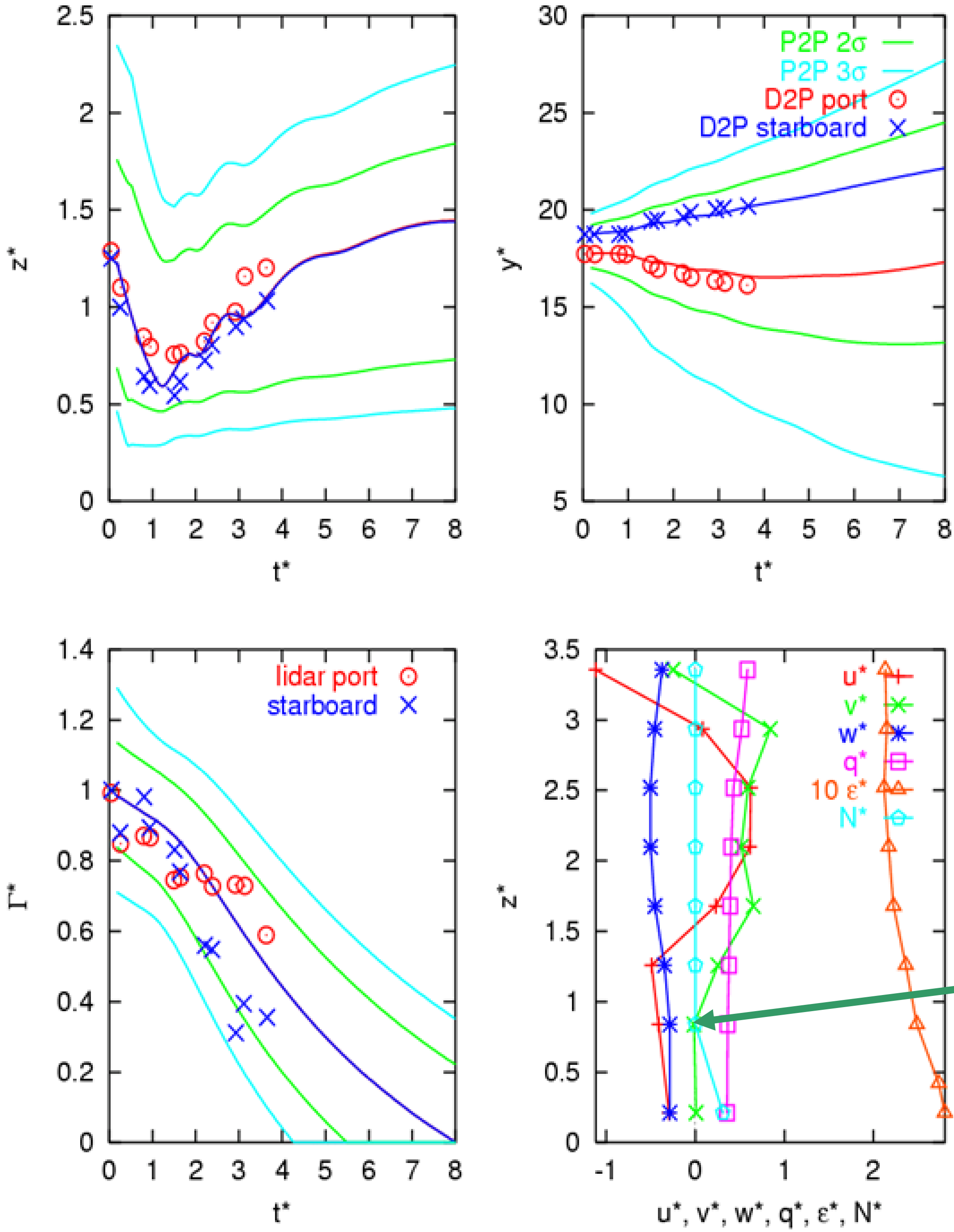

application examples

minor crosswind

⇒ symmetric rebound

v*~0

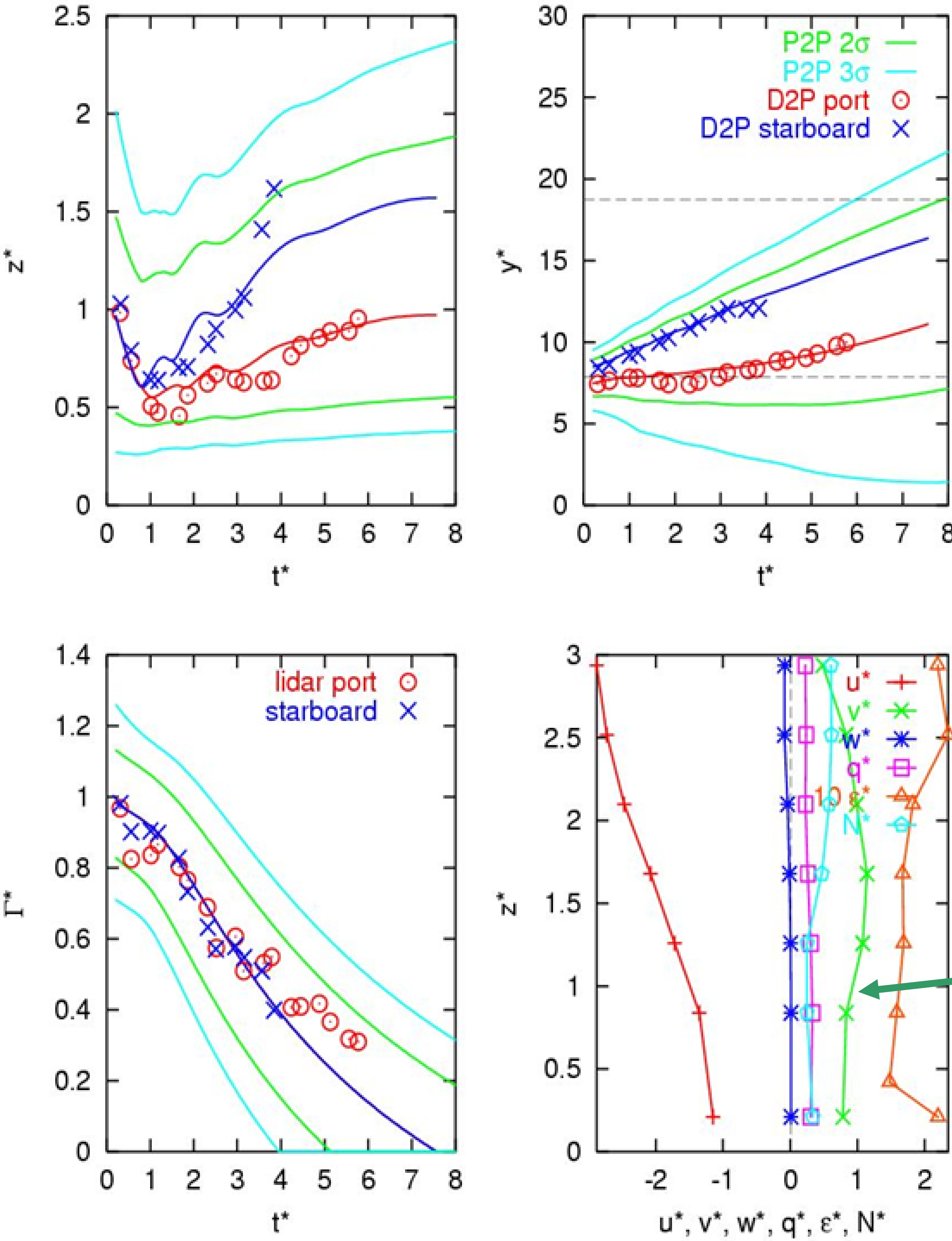

application examples

weak crosswind

⇒ asymmetric rebound

$v^* \approx 1$

application examples

behaviour near obstacles

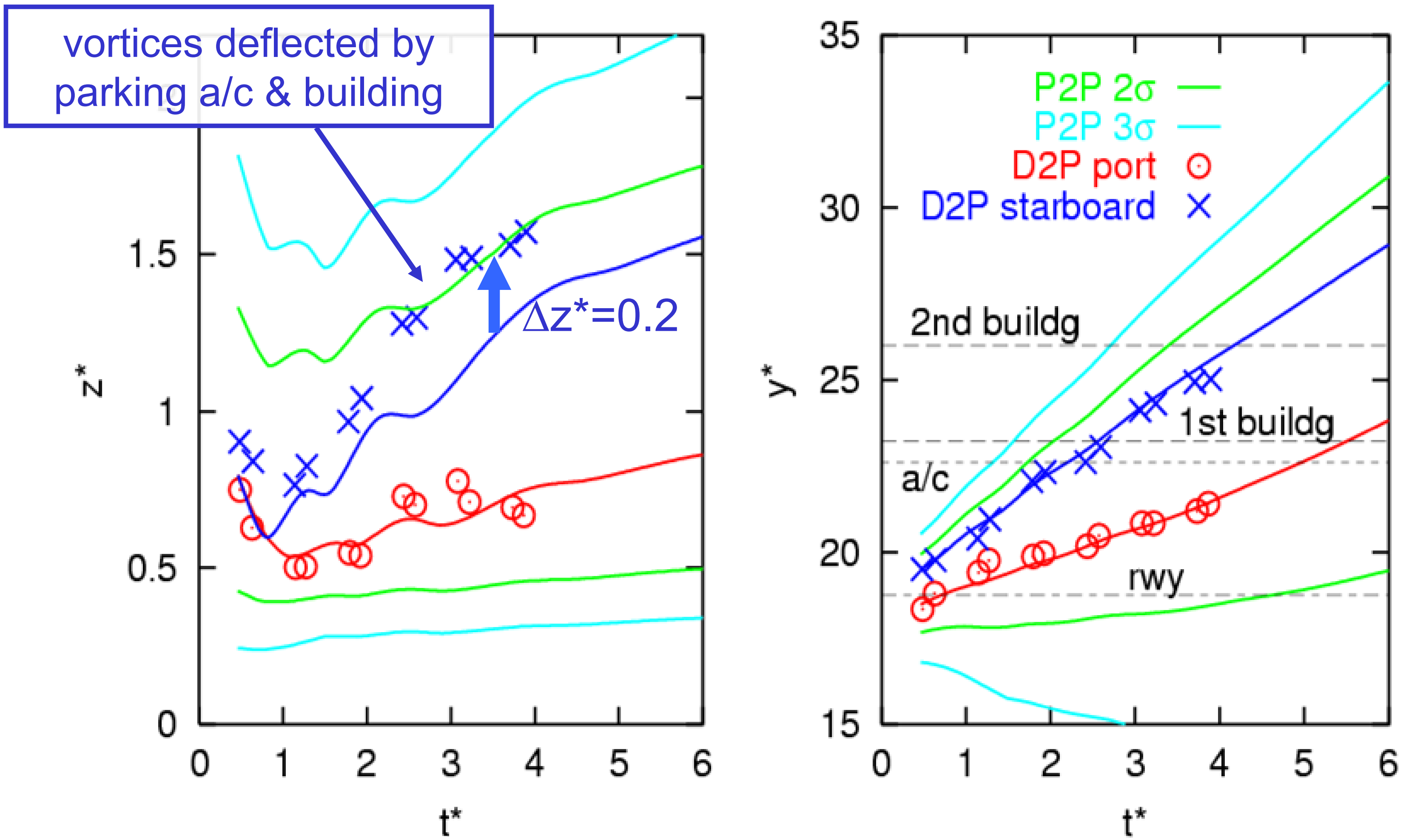

$v^* = 1.5$, $z_{building} = 9.7$ m $\Rightarrow \Delta z^*=0.2$

Holzäpfel & Steen, AIAA J. **45** 2007

application examples –

exceptional WV rebound due to shear layers

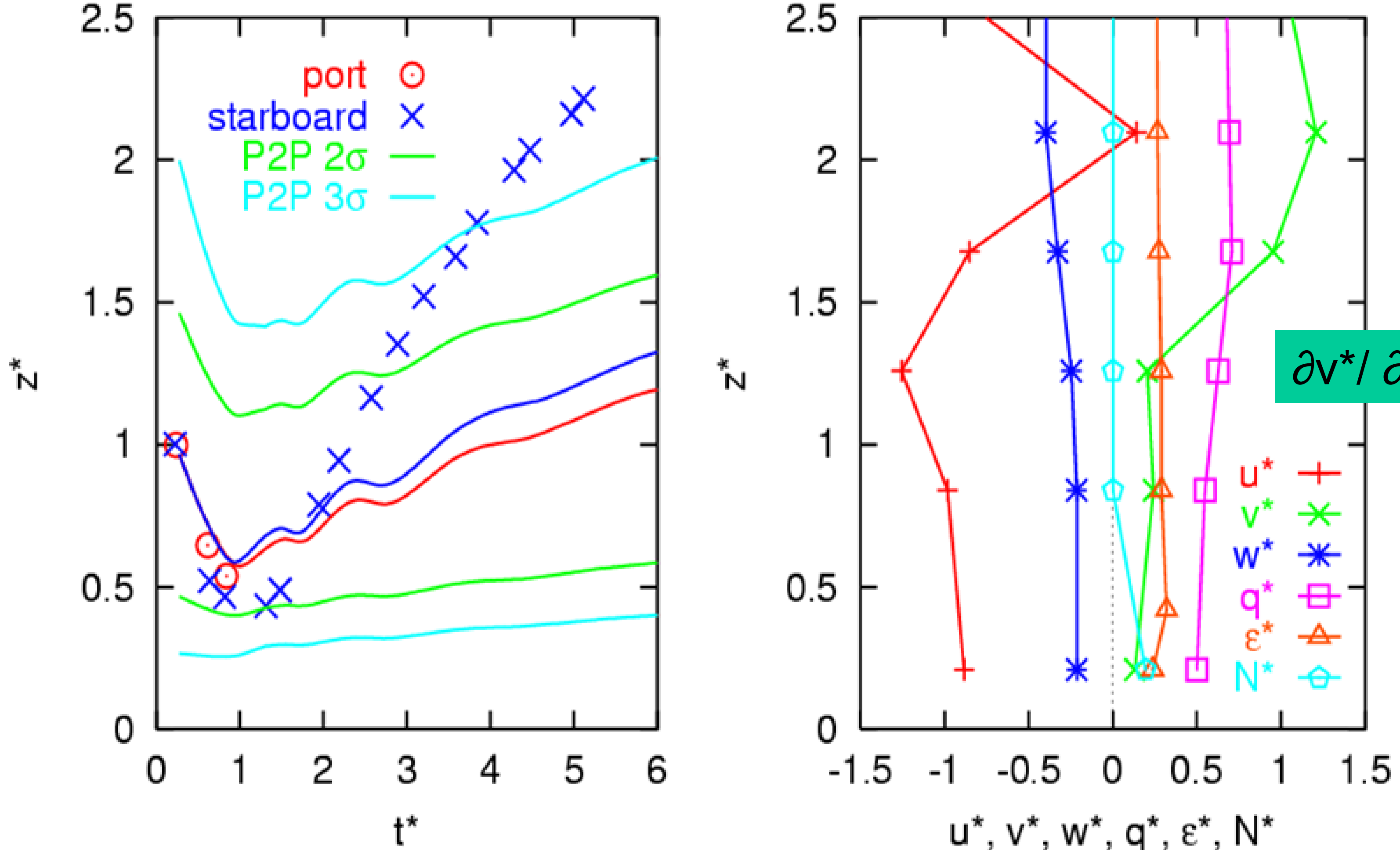

wake generation below b_0 ($z_{0,min} = 0.1\ b_0$)

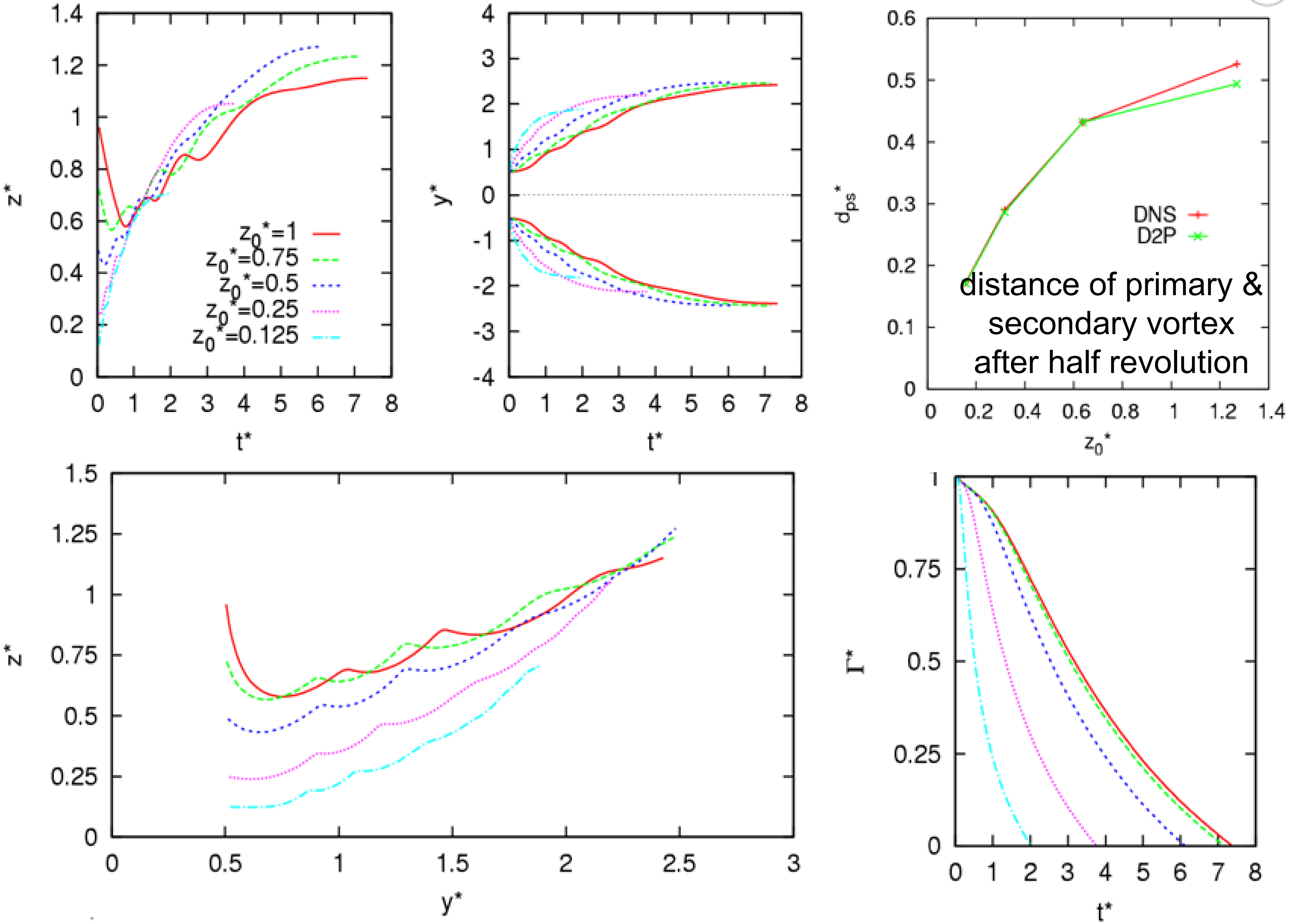

Probabilistic concept – 3 layers

fixed uncertainties:

- variation of decay parameters $(\upsilon^*_{2,u}, 0.8T^*_2); (\upsilon^*_{2,l}, 1.2T^*_2)$
- uncertainty allowances $\pm b_0, \quad \pm 0.2\Gamma_0$

dynamic uncertainties:

- uncertainty allowances $y^*_{u(l)}, z^*_{u(l)} = y^*, z^* + (-)\int \sqrt{\left(C_q q^*\right)^2 + \left(C_{sh} v^*_{sh}\right)^2}\, dt^*$

model calibration with measurement data:

- uncertainty allowances (see next slide)

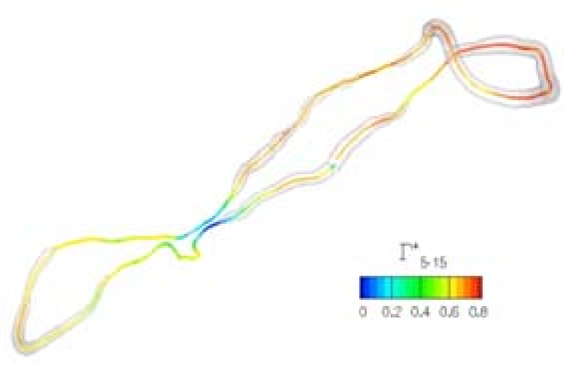

Model Calibration with Measurement Data

prediction of envelopes with defined probabilities

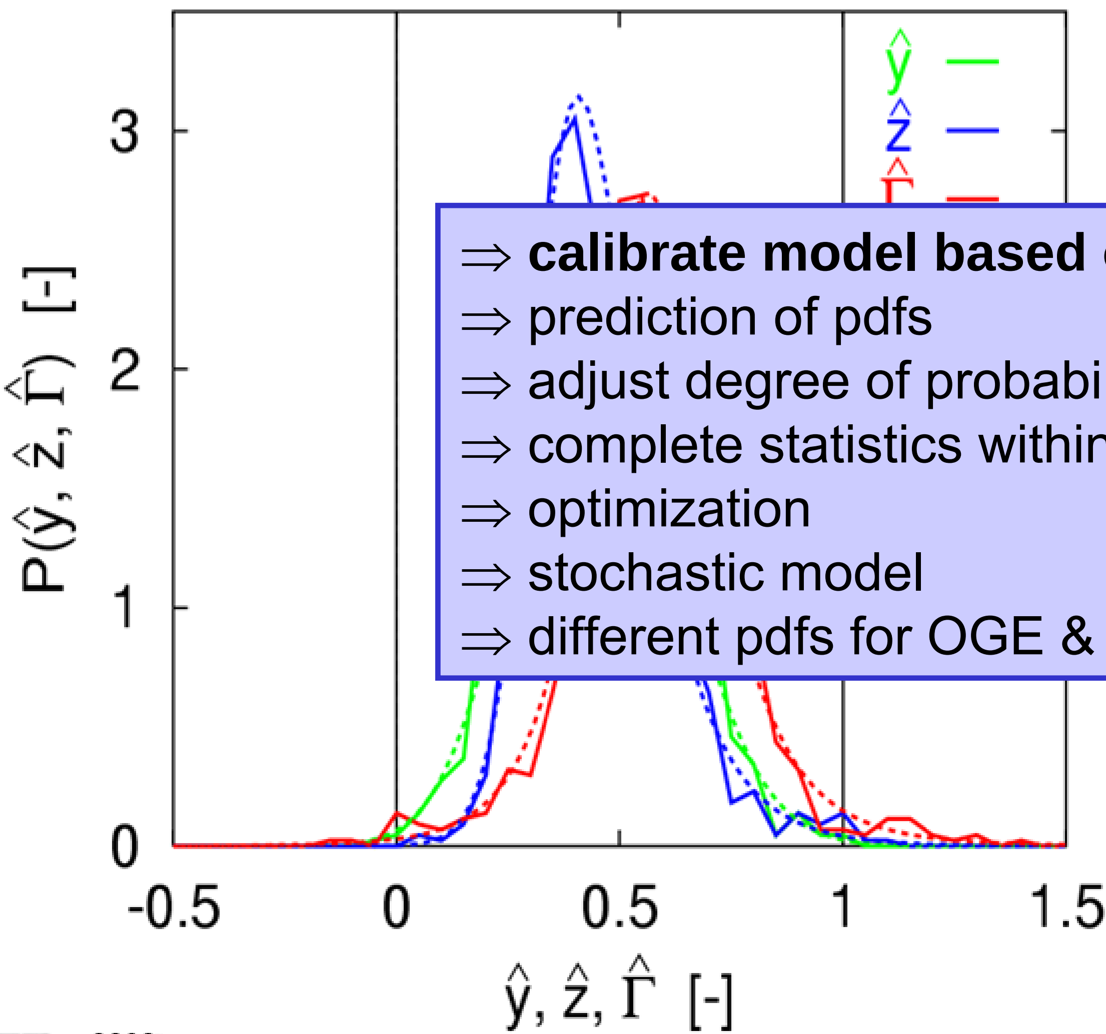

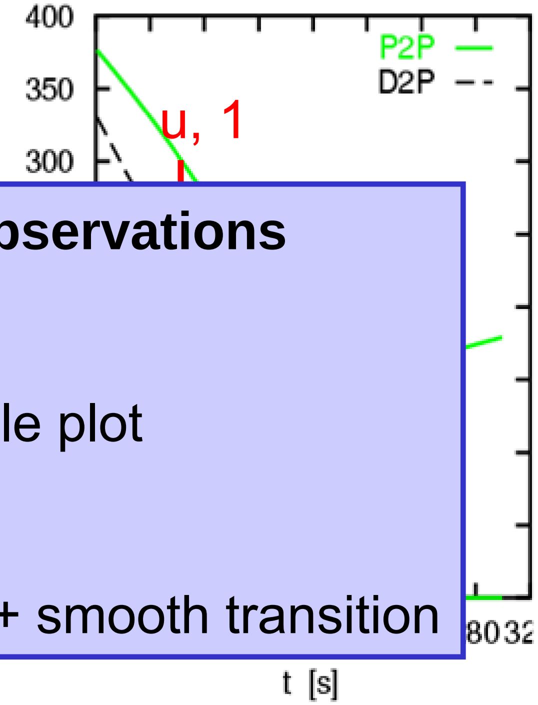

- ⇒ **calibrate model based on observations**
- ⇒ prediction of pdfs
- ⇒ adjust degree of probability
- ⇒ complete statistics within single plot
- ⇒ optimization
- ⇒ stochastic model
- ⇒ different pdfs for OGE & IGE + smooth transition

$$\hat{z} = \frac{z_{meas} - z_l}{z_u - z_l}$$

Holzäpfel, J. Aircraft **43** 2006

probabilistic / stochastic prediction modes

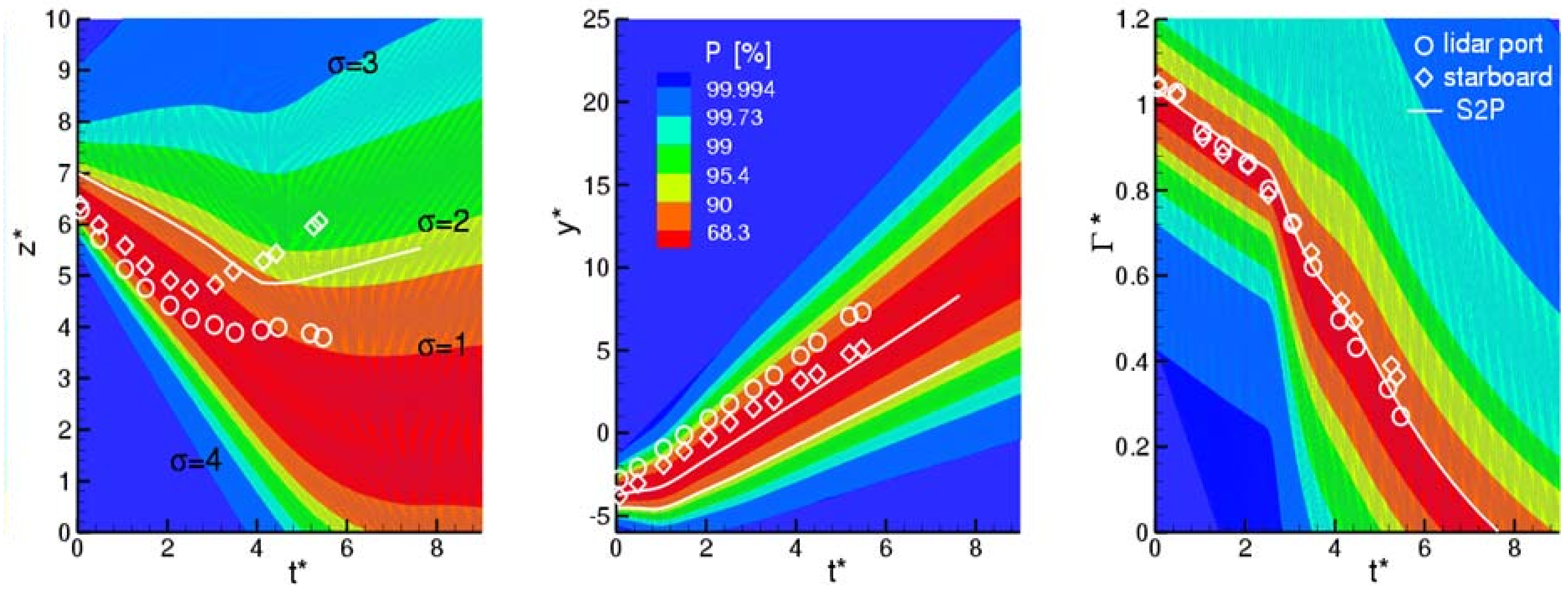

P2P validation work - survey

campaign	No. cases	det./prob. scoring	compared to	a/c types	flight phases	documentation
Memphis, TN (1994, 1995)	282 211	X/-	APA	23 hvy/med/li	arrival OGE/IGE	J. Aircraft 2003/2004
Dallas Fort Worth, TX (1997)	191	X/-		16 hvy/med/li	arrival OGE/NGE	J. Aircraft 2004
WakeOP (2001)	41	X/-	APA	ATTAS	level/hi-lift OGE	J. Aircraft 2004
WakeTOUL Tarbes (2002)	32	X/X	APA	A340	lev/arr/cl/hi OGE	J. Aircraft 2006
AWIATOR FT1 Tarbes (2003)	32	X/X	APA	A340	level/take-off/OGE	J. Aircraft 2006
WakeFRA Frankfurt (2004)	282 + 233	X/X	APA / DVM	25 hvy/med	arrival IGE/OGE	AIAA J. 2007
CREDOS EDDF-1 (2007)	137	X/-	DVM	12 heavy	departure OGE	CREDOS D2-3, 2008
CREDOS EDDF-2 (2007)	~ 9,000	X/-	DVM	28 med/hvy	departure IGE/NGE	CREDOS D2-3, 2009
unpublished					cruise/arr. OGE/IGE	

Comparison with other WV models

example D2P & DVM (CREDOS)

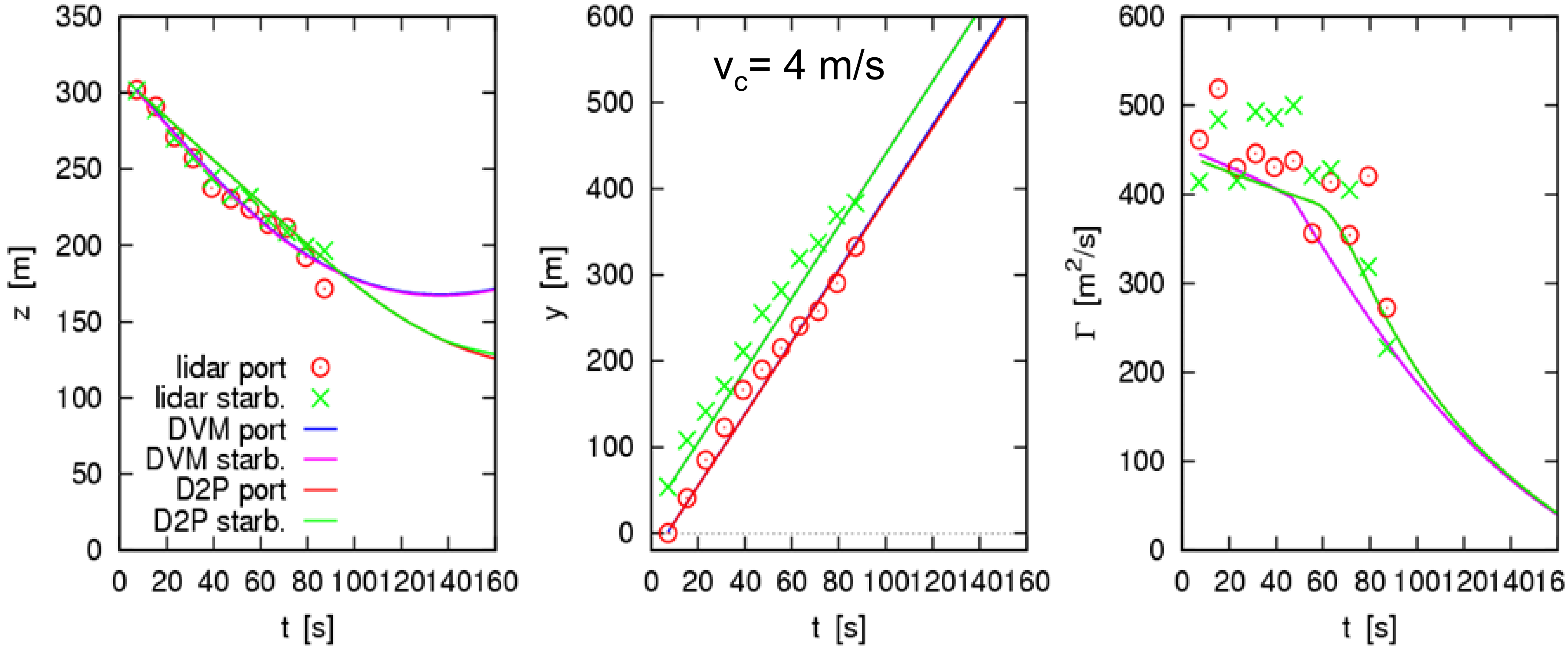

Prediction Skill

deterministic scoring results

model with perfect (MET) data would be much better

	RMS $\Delta\Gamma_{5-15} / \Gamma_0$	RMS $\Delta z \,/\, b_0$	RMS $\Delta y \,/\, b_0$
best median	0.128	0.118	0.402
worst median	0.240	0.452	0.968

worst median	86 m²/s	17 m	34 m

application examples

long-lived vortex rings

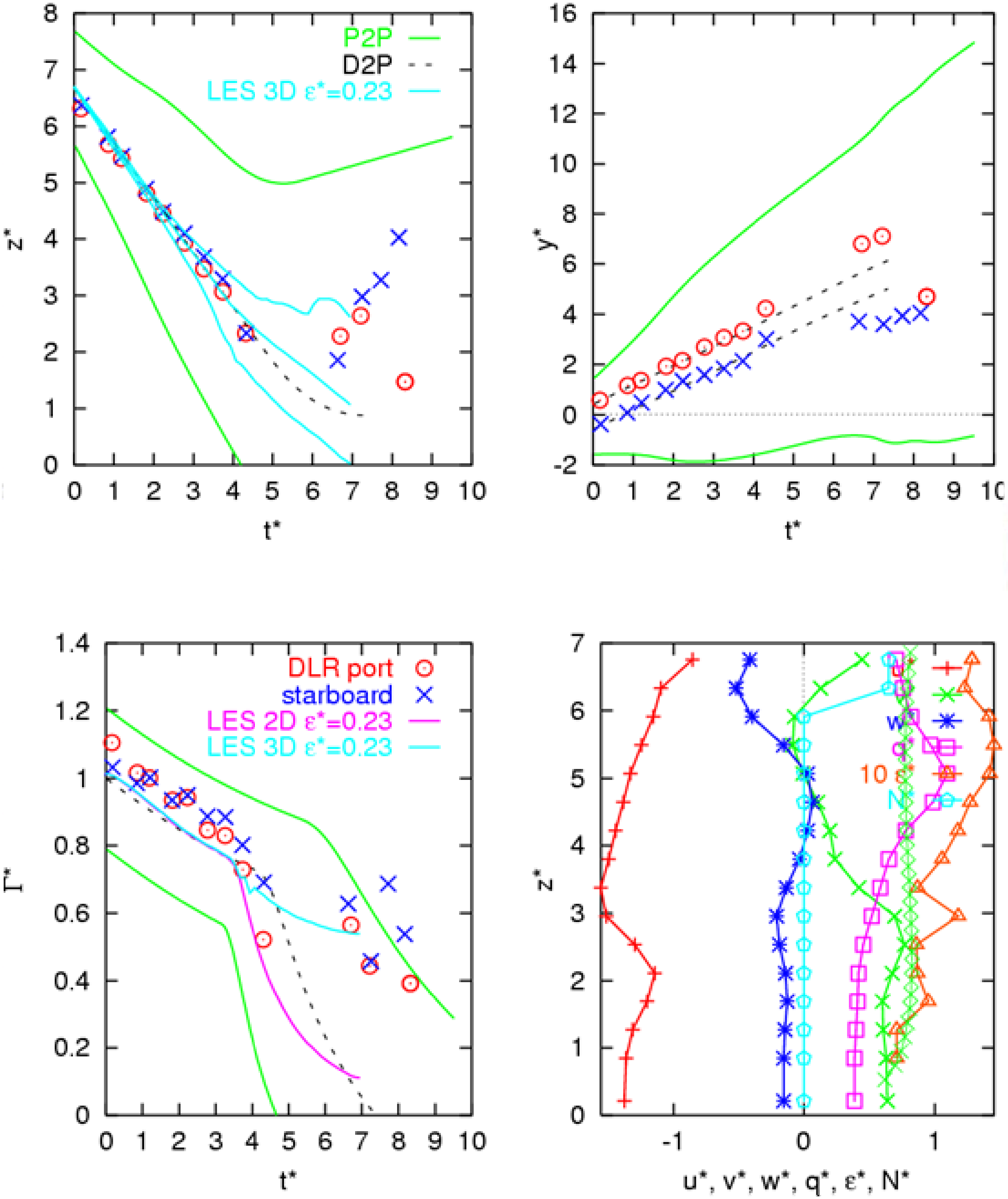

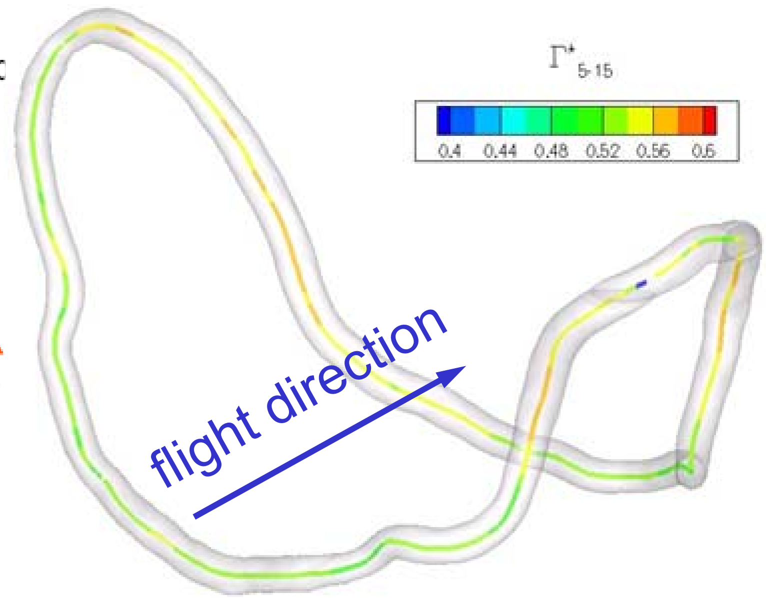

Hennemann & Holzäpfel, 5th Int. Symp. Turbulence & Shear Flow Phenomena, TU Munich 2007

circulation decay – vortex topology

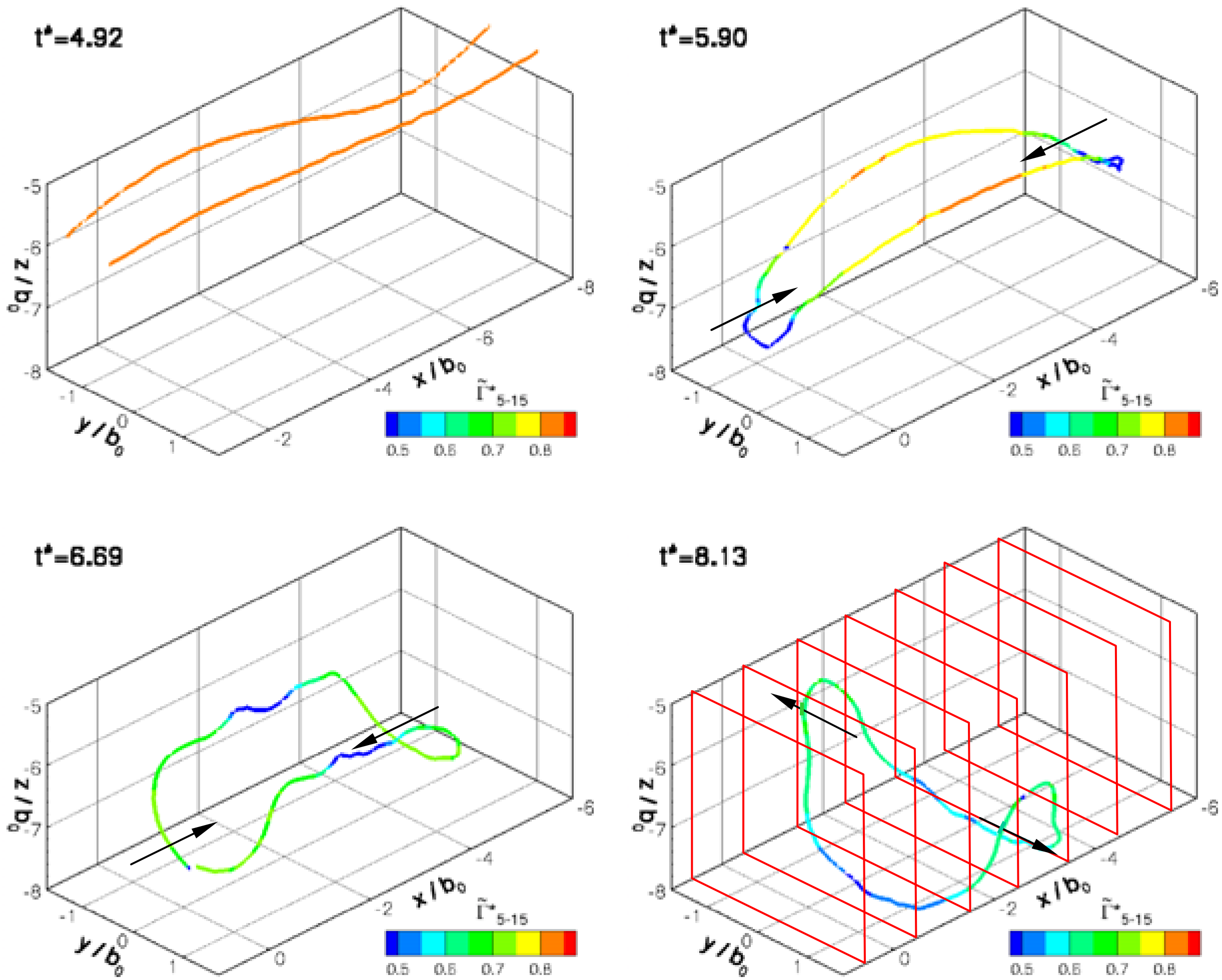

- 2-phase decay: shortening of vortex segments in flight direction
- topology caused by mutual velocity induction
- redistribution of $\Gamma_{5\text{-}15}$ by vortex stretching and compression and / or collision of pressure waves

$\varepsilon^* = 0.05$, $N^* = 0$, $L_t^* = 0.41$

circulation decay characteristics

continuous to 3-phase decay

LESTUF

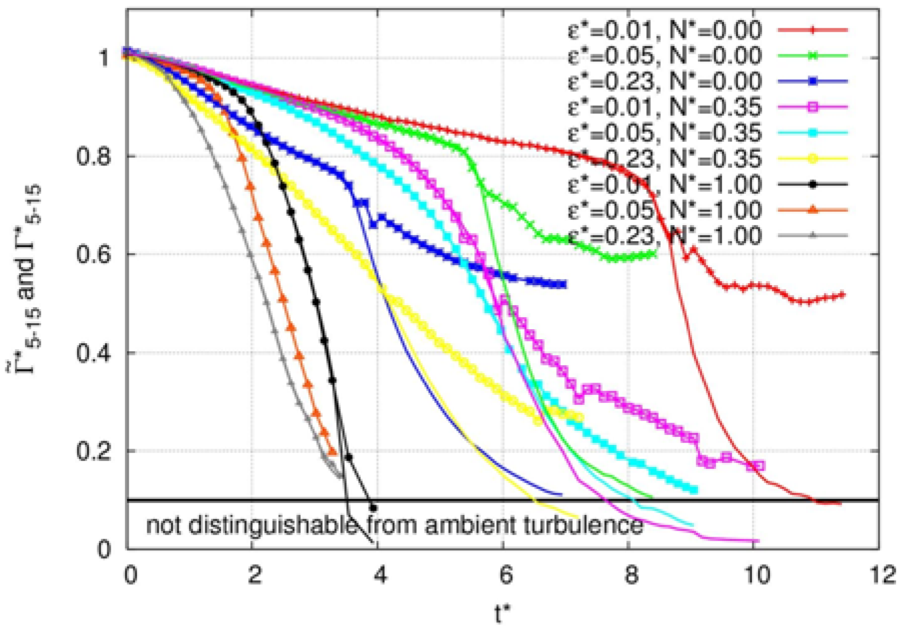

MGLET

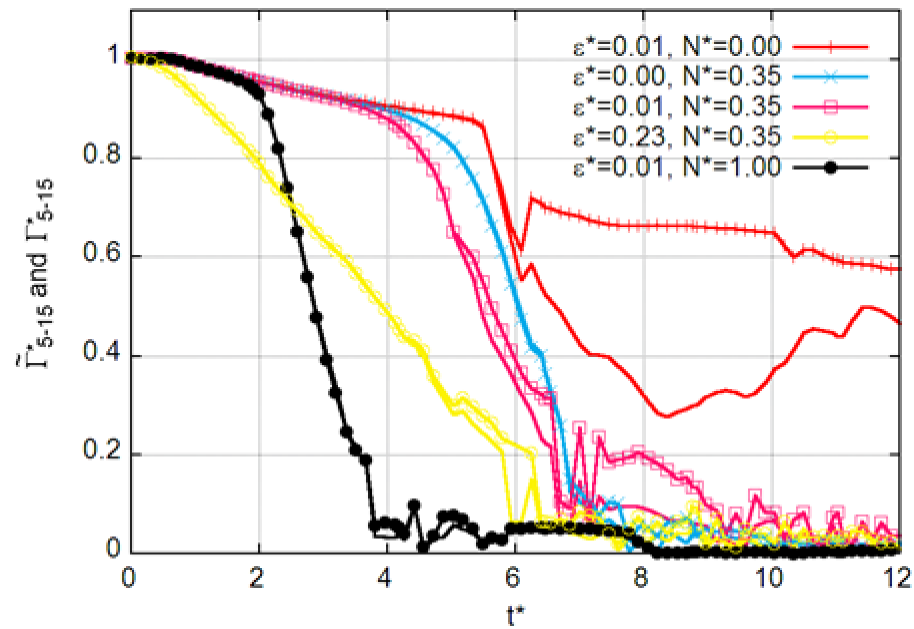

- good agreement in stable stratification – large uncertainties in neutral strat.
- neutral - weak stratification: three-phase decay of circulation to vortex line:

  diffusion phase – rapid decay phase – ring diffusion phase

P3P – long-lived vortex rings, L_t

preliminary results (Ingo Hennemann)

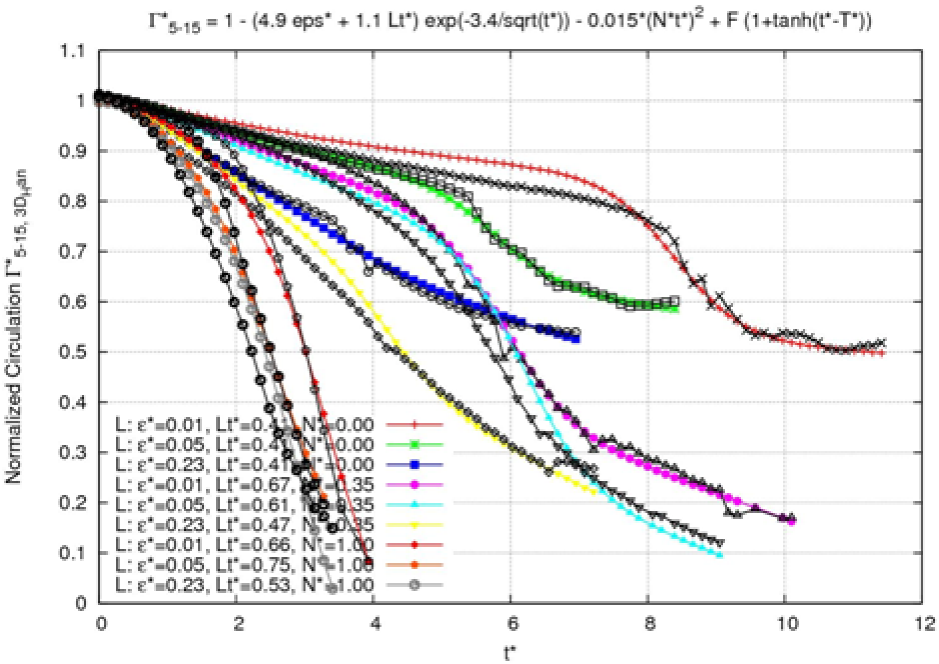

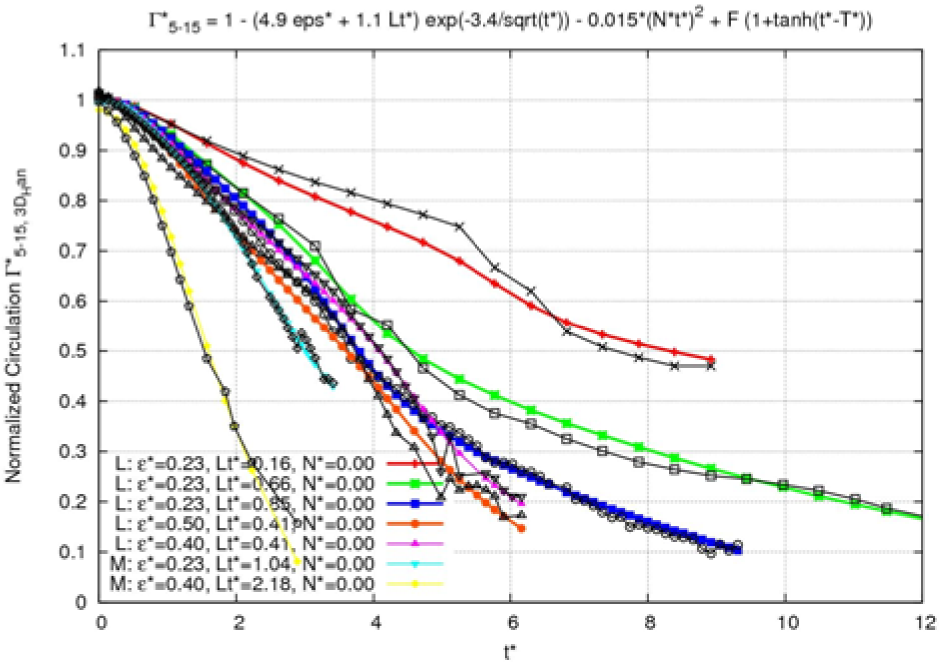

$$\Gamma^*_{5-15} = 1 - \left(4.9\varepsilon^* + 1.1L^*_t\right)\exp\frac{-3.4}{\sqrt{t^*}} - 0.015\left(N^*t^*\right)^2 + C\left(1 + \tanh(t^* - T^*)\right)$$

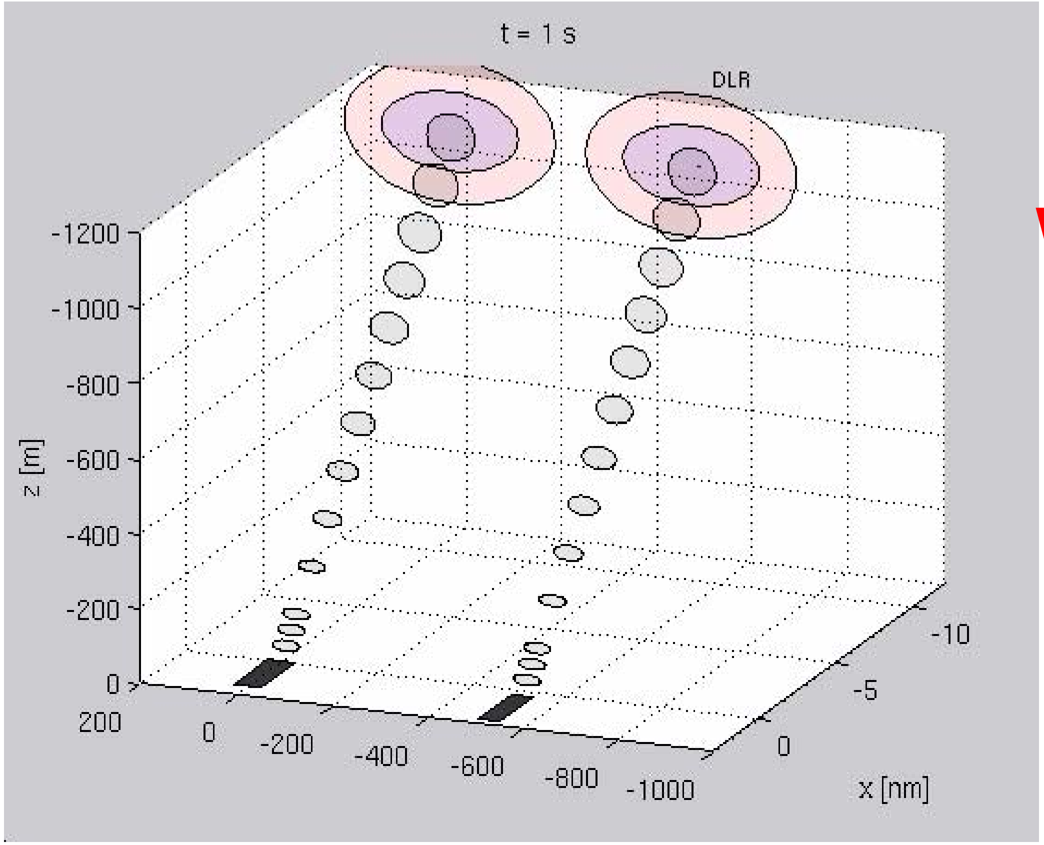

Wake Vortex Prediction & Monitoring System WSVBS

strong crosswind

2004/09/10 19:10

prediction of weather dependent aircraft separations for approach and landing

WakeScene – sensitivity analysis, risk assessment

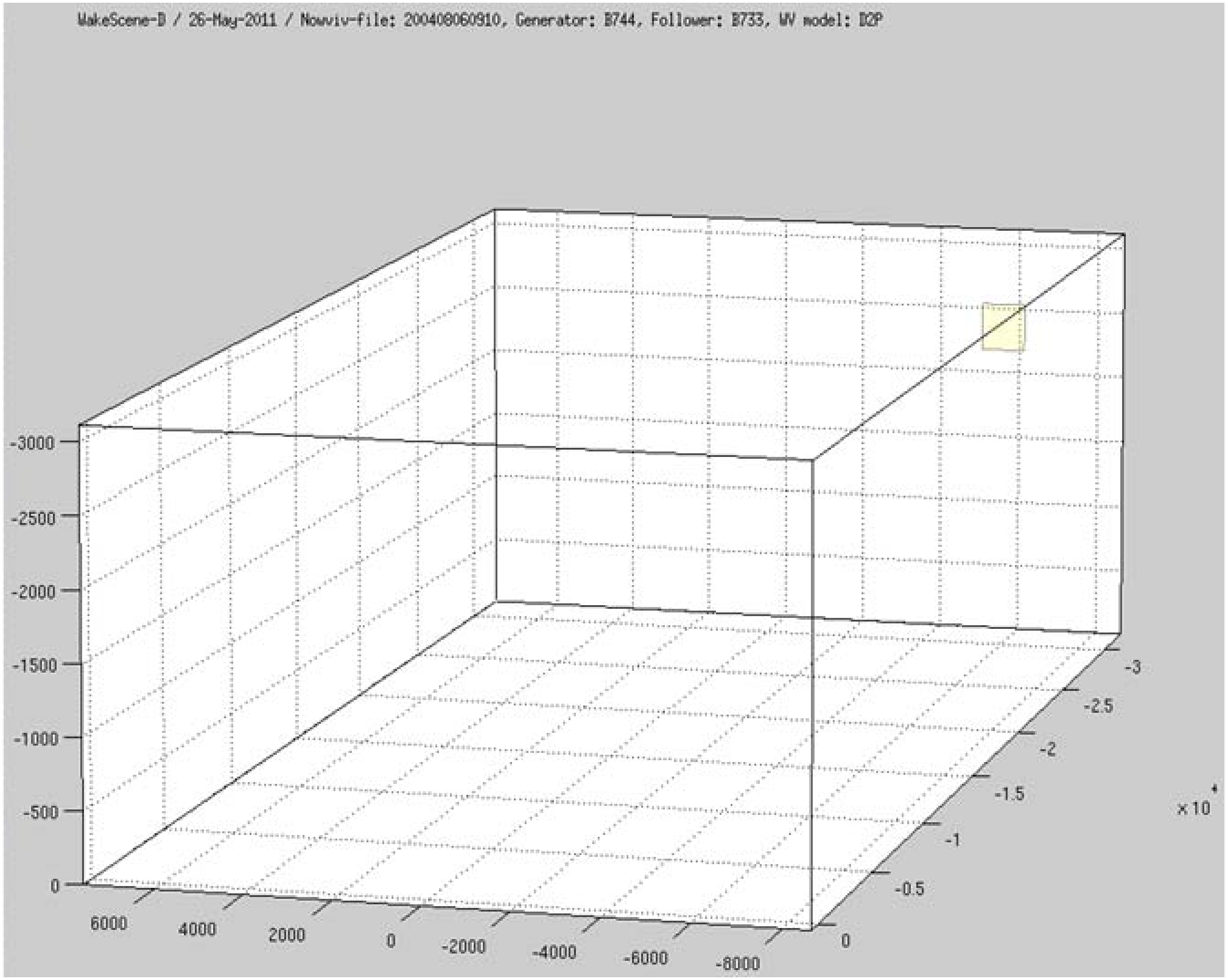

Holzäpfel et al., Aircraft Wake Vortex Scenarios Simulation Package - WakeScene, Aerospace Science and Technology **13,** 2009.
Holzäpfel et al., Aircraft Wake Vortex Scenarios Simulation for TakeOff and Departure, Journal of Aircraft **46**, 2009, 713-717.
Holzäpfel & Kladetzke, Assessment of Wake Vortex Encounter Probabilities for Crosswind Departure Scenarios, J. Aircraft **48**, No. 3, 2011.

WakeScene-D ⇔ field measurements EDDF-2

lateral WV transport in Lidar plane (~10.000 departures)

EDDF-2 WakeScene-D

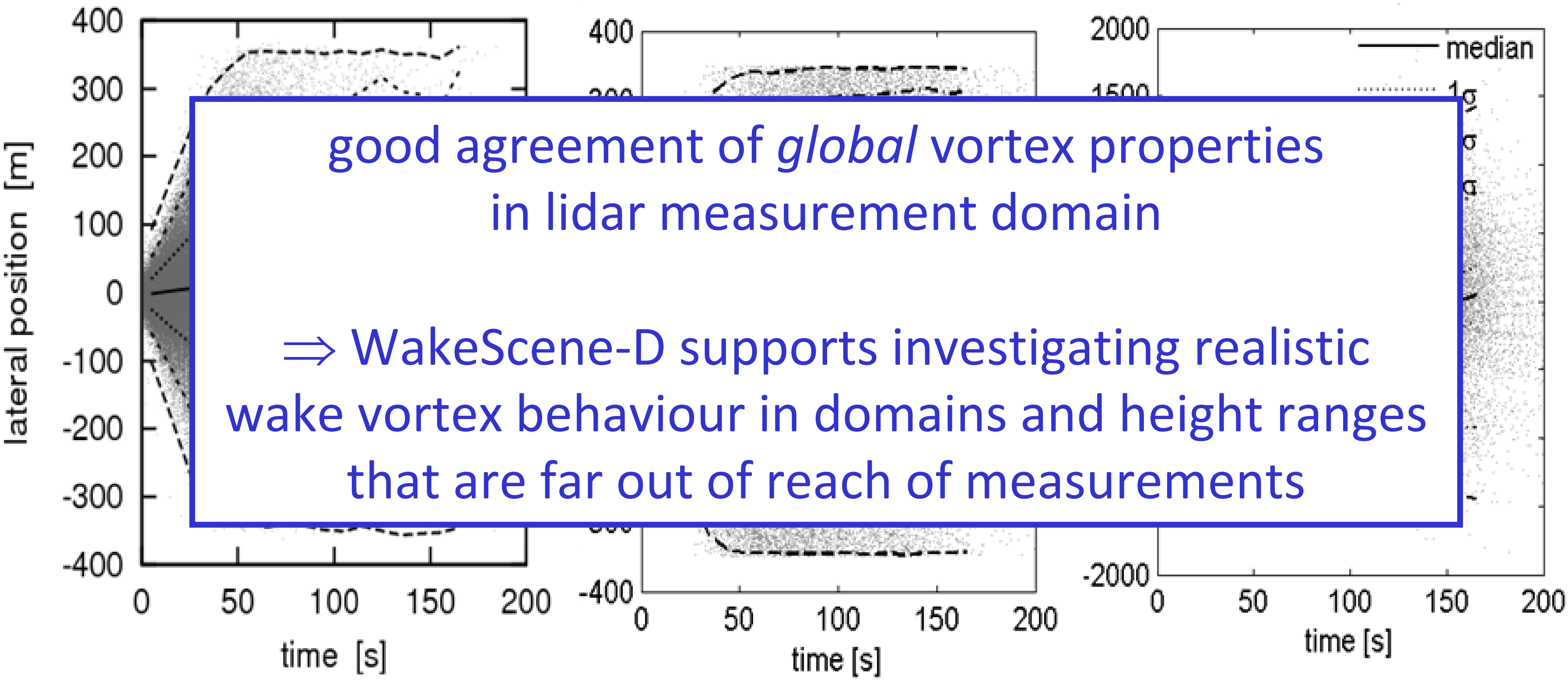

measurement domain zoom on lidar domain full domain

good agreement of *global* vortex properties
in lidar measurement domain

⇒ WakeScene-D supports investigating realistic
wake vortex behaviour in domains and height ranges
that are far out of reach of measurements

contribution of contrail cirrus to global warming

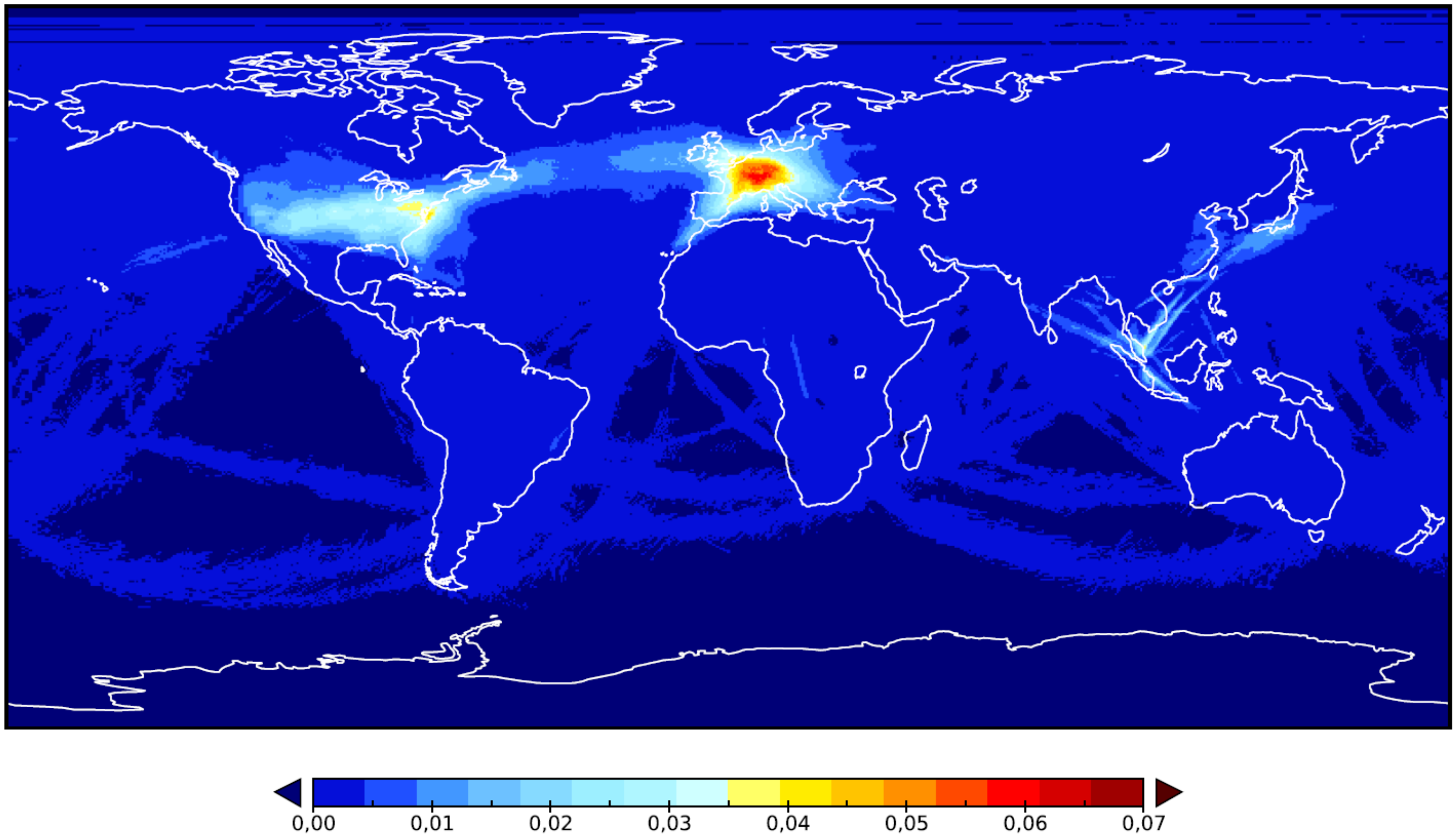

Annual mean solar optical depth of the sum of contrails computed with CoCiP for the year 2006

Schumann, Graf, Mannstein, AIAA Paper 2011-3376

contribution of contrails to global warming

maximum WV descent distances

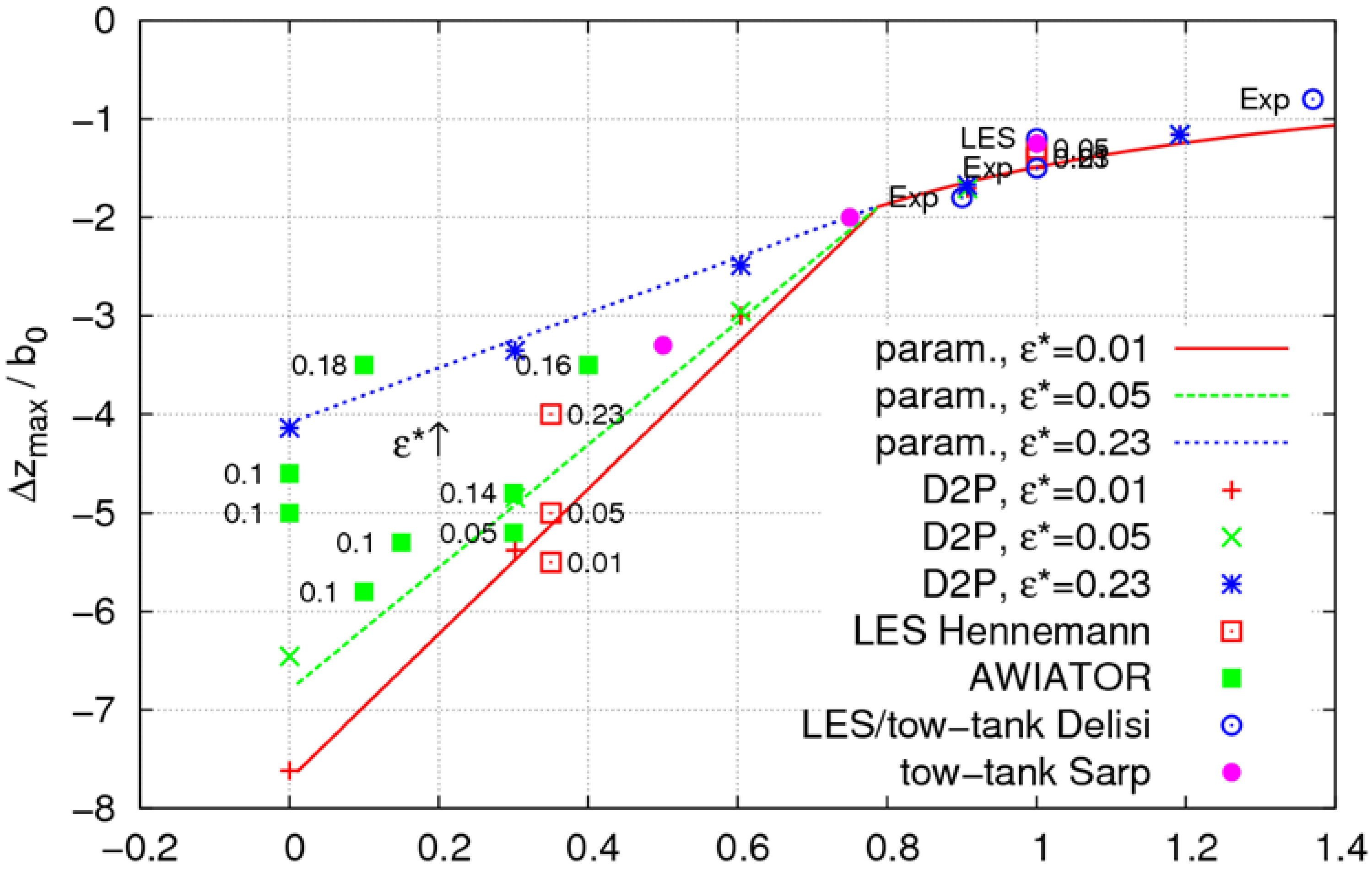

Δz*

Δz*

- robust for stable stratification
- substantial uncertainties for neutral stratification

0.36

P2P – References / Applications

- F. Holzäpfel, "Probabilistic Two-Phase Wake Vortex Decay and Transport Model", J. Aircraft **40,** 323-331, 2003.
- F. Holzäpfel F., R.E. Robins, "Probabilistic Two-Phase Aircraft Wake-Vortex Model: Application and Assessment", J. Aircraft **41**, 1117-1126, 2004.
- F. Holzäpfel, "Probabilistic Two-Phase Aircraft Wake-Vortex Model: Further Development and Assessment", J. Aircraft **43**, 700-708, 2006.
- F. Holzäpfel, M. Steen, "Aircraft Wake-Vortex Evolution in Ground Proximity: Analysis and Parameterization", AIAA J. **45**, 218-227, 2007.
- M. Frech, F. Holzäpfel, "Skill of an aircraft wake-vortex transport and decay model using short-term weather prediction and observation", J. Aircraft **45**, 461-470, 2008.

WSVBS, ATC-Wake , SESAR 12.2.2, WakeScene, OWBPA, WEPS, CoCiP, WaVoP

coded (partly) by 12 other groups

Conclusions & Outlook

- accounts for relevant effects of aircraft and atmosphere
- prediction of probabilistic uncertainty allowances (pdfs)
- good prediction skill
- comprehensive comparison with field measurement data & other models
- fast (P2P 0.01 s, runtime optimized D2P version OGE 0.001 s on PC)

- consideration of long-lived rings and turbulence length scale
- refinement of ground effect modeling employing measurements at Munich airport and LES of Anton Stephan

Wake Vortex Advisory System “WSVBS”

supports weather dependent dynamic a/c separations

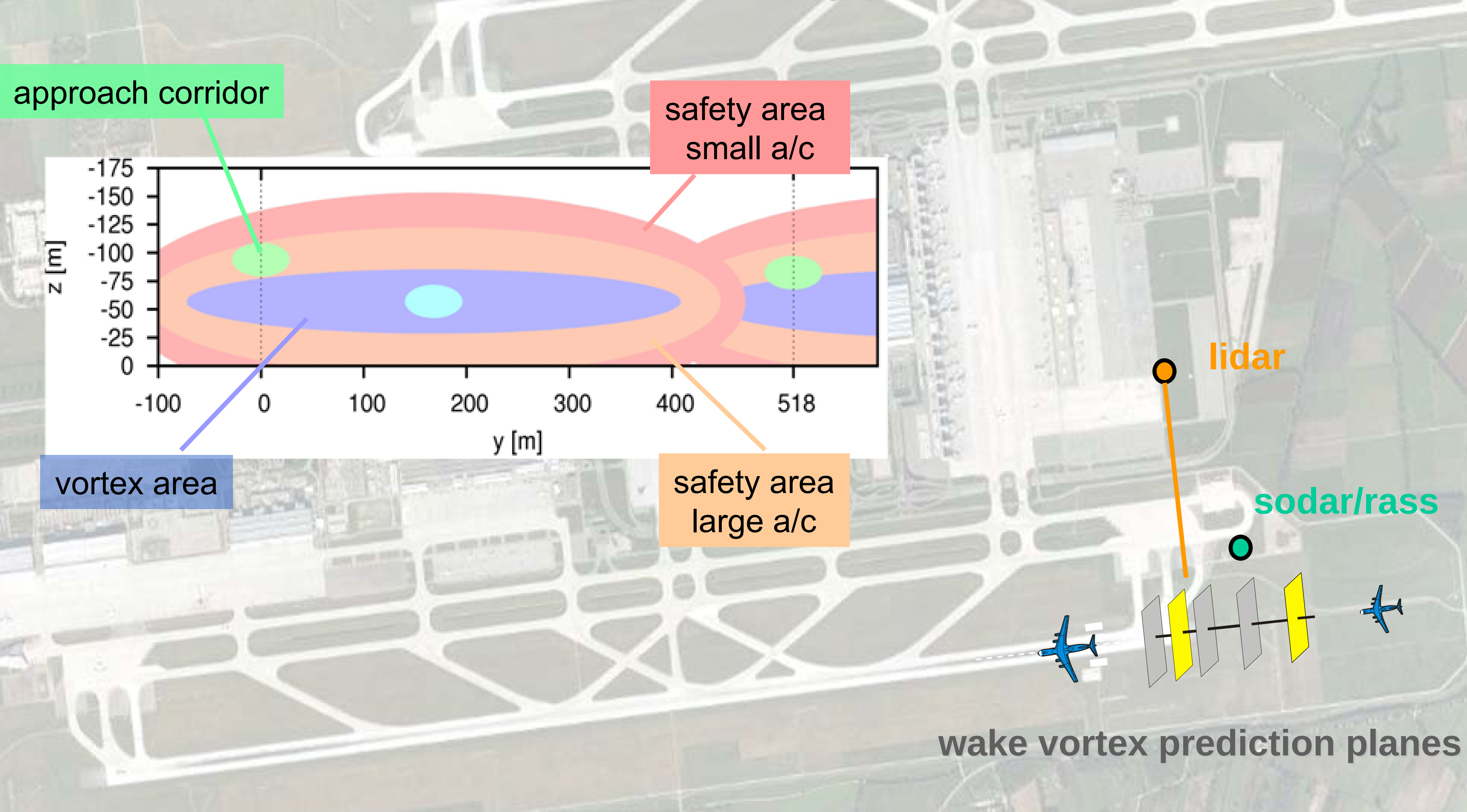

Air Traffic Control Quarterly, Vol. 17, No. 4, 2009